Research Square

Preprints are preliminary reports that have not undergone peer review.
They should not be considered conclusive, used to inform clinical practice,
or referenced by the media as validated information.

Anaerobic gut fungi enhance bioplastic degradability under anaerobic digestion conditions

Colleen B. Ahern
University of California, Santa Barbara
Malte Herold
Luxembourg Institute of Science and Technology
Shirley Jin
University of California, Santa Barbara
Ramya Ragunathan
University of California, Santa Barbara
Hugh M. Purdy
University of California, Santa Barbara
Bo Zhang
University of California, Santa Barbara
Iikpoemugh Elo Imiete
Luxembourg Institute of Science and Technology
Elaina Blair
University of California, Santa Barbara
Michelle A. O'Malley
University of California, Santa Barbara
Magdalena Calusinska
magdalena.calusinska@list.lu

Luxembourg Institute of Science and Technology

Research Article

Keywords: Anaerobic digestion, anaerobic gut fungi, bioplastics biodegradation, microbiome, metatranscriptomics, transcriptomics, CAZymes

Posted Date: November 17th, 2026

DOI: https://doi.org/10.21203/rs.3.rs-11759486/v1

License: This work is licensed under a Creative Commons Attribution 4.0 International License.
Read Full License

Additional Declarations: No competing interests reported.

Anaerobic gut fungi enhance bioplastic degradability under anaerobic digestion conditions

Authors/Affiliations: Colleen B. Ahern[1], Malte Herold[2], Shirley Jin[1], Ramya Ragunathan[1], Hugh M. Purdy[1], Bo Zhang[1], Iikpoemugh Elo Imiete[2], Elaina M. Blair[1], Michelle A. O'Malley[1,3,4**], Magdalena Calusinska[1,2**]

[**] Corresponding Authors

Author information

[1]Department of Chemical Engineering, University of California, Santa Barbara, CA 93106, USA
Colleen B. Ahern (colleen_ahern@ucsb.edu), Shirley Jin (jin18@ucsb.edu), Ramya Ragunathan (r_ragunathan@ucsb.edu), Hugh M. Purdy (hmpurdy@ucsb.edu), Bo Zhang (bozhang@ucsb.edu), Elaina M. Blair (elainablair@ucsb.edu), Michelle A. O'Malley (momalley@ucsb.edu), Magdalena Calusinska (magdalena.calusinska@list.lu)
[2]Environmental and Industrial Biotechnologies Unit, Luxembourg Institute of Science and Technology, Hautcharage, L-4940, Luxembourg
Malte Herold (malte.herold@list.lu), Iikpoemugh Elo Imiete (iikpoemughelo.imiete@list.lu)
[3]Joint BioEnergy Institute (JBEI), Emeryville, CA, 94608, USA
[4]Department of Bioengineering, University of California, Santa Barbara, CA 93106, USA

[**] Corresponding Authors

Michelle A. O'Malley and Magdalena Calusinska

Keywords

Anaerobic digestion, anaerobic gut fungi, bioplastics biodegradation, microbiome, metatranscriptomics, transcriptomics, CAZymes

Abstract

Background

Biodegradable bio-based plastics (BPs) were developed to mitigate environmental plastic pollution, but they generally degrade more readily under aerobic than anaerobic conditions. Aerobic composting produces carbon dioxide, while anaerobic digestion (AD) generates both CO_2 and methane. Because CH_4 is a valuable energy source, enhancing plastic biodegradation under AD conditions could both reduce plastic waste and support fuel production. This study investigates anaerobic gut fungi (AGF) as a biological pretreatment enhancing the biodegradability of different bioplastic designs within AD sludge microbiomes.

Results

Three AGF-BP pairings were chosen to evaluate the efficacy of AGF pretreatment in improving BP biodegradability in anaerobic sludge. A polyhydroxyalkanoate (PHA) straw was pretreated with *Neocallimastix californiae*, while cellulose acetate (CA) and polylactic acid (PLA) films were pretreated with *Neocallimastix lanati*. Measurements of biogas production, BP weight loss, and surface characterization demonstrated that *N. californiae* enhanced the biodegradability of PHA and *N. lanati* enhanced the biodegradability of CA, whereas *N. lanati* did not significantly improve PLA biodegradability under AD conditions. 16S rRNA gene amplicon sequencing and metatranscriptomic analyses showed that the AGF-pretreated PHA and CA induced significant, BP-specific shifts in the relative abundance of microbial taxa, carbohydrate-active enzyme (CAZyme) transcripts, and other functional genes within the AD microbiome. Furthermore, biogas measurements revealed that *N. lanati* could partially metabolize CA during the pretreatment phase, but *N. californiae* could not metabolize PHA. These findings suggest that *N. lanati* acts through both enzymatic and mechanical mechanisms on CA, while *N. californiae* likely functions primarily through mechanical disruption of PHA. Transcriptomic analysis of *N. lanati* during the pretreatment phase further revealed upregulation of cellulolytic CAZymes and adhesion-related genes when grown on CA, suggesting that these factors likely contribute to CA degradation.

Conclusions

Our findings show for the first time that AGF pretreatment enhances biodegradability of BPs under AD conditions, likely through a synergistic effect of enzymatic hydrolysis and mechanical disruption of the polymer structure. These results highlight AGF as a promising biological pretreatment strategy for enhancing energy recovery and carbon valorization from bioplastic waste streams.

Background

It is estimated that the amount of global plastic waste more than doubled from 156 million tons (Mt) in 2000 to 353 Mt in 2019 [1]. One response to this growing issue has been the development of biodegradable polymers that shall completely break down in the environment after disposal. Several types of standardized tests, including the American Society for Testing and Materials (ASTM), International Organization for Standardization (ISO), and European Standards (EN) methods, assess the biodegradability of such polymers under different operating and environmental conditions. Polymer biodegradation is commonly assessed under aerobic composting conditions, in which microbial mineralization produces carbon dioxide (CO_2) [2]. Under anaerobic digestion (AD) conditions, mineralization can produce both CO_2 and methane (CH_4), with the latter representing a recoverable energy carrier [3]. Therefore, for polymers that are biodegradable under AD conditions, AD may offer a route for simultaneous waste treatment and energy recovery. However, many polymers exhibit limited or slow biodegradation under anaerobic conditions, often with lower mineralization rates or extents than under aerobic composting conditions [4]. In addition, reported anaerobic biodegradation performance varies substantially among studies as a result of differences in operating conditions, inoculum characteristics, and test protocols [5,6]. This variability limits the comparability and predictability of polymer biodegradation in AD systems.

Due to these limitations on anaerobic polymer biodegradation, it is advantageous to apply pretreatments to polymers that increase their biodegradability under more diverse conditions. Physical, thermal, chemical, and biological pretreatment methods have been shown to enhance the biodegradation of certain polymer designs [7]; however, such pretreatments must be inexpensive and sustainable to be implemented at a large scale. Biological systems have therefore emerged as strong candidates for such applications due to their environmentally friendly nature. Fungi in particular have been shown to substantially contribute to polymer biodegradation due to their wide array of secreted degradative enzymes. However, these studies [8] are often limited to aerobic fungi because of their strong oxidative mechanisms, leaving anaerobic fungi underexplored in this area of research.

Anaerobic gut fungi (AGF) are members of large herbivore gut microbiomes that play a key role in digesting lignocellulosic biomass, which is largely driven by their secretion of carbohydrate-active enzymes (CAZymes) [9,10]. CAZymes drive the degradation, modification, and assembly of carbohydrates and are classified into the six following classes: glycoside hydrolases (GHs), glycosyltransferases (GTs), polysaccharide lyases (PLs), carbohydrate esterases (CEs), carbohydrate-binding modules (CBMs), and auxiliary activities (AAs) [11,12]. AGF genomes encode more copies of CAZymes than other fungi commonly used in industrial applications [13], and they organize their CAZymes into large multi-enzyme complexes known as cellulosomes, which enhance their degrading power [14]. These features, along with their ability to develop invasive rhizoid structures that penetrate biomass, enable AGF to physically and enzymatically disrupt plant cell walls and accelerate lignocellulose hydrolysis [15,16]. Collectively, these

characteristics position AGF as strong candidates for degrading recalcitrant substrates beyond lignocellulose, including synthetic plastics. While AGF have so far been shown to metabolize various types of lignocellulosic biomass under anaerobic conditions [17,18], their potential to enhance plastic degradation has not yet been evaluated.

Previously, several types of PHA have been shown to biodegrade under AD conditions, whereas CA and PLA are not recognized as readily biodegradable in AD systems [19–21]. In this study, we assessed the ability of two previously isolated AGF strains, *Neocallimastix californiae* (G1) [14] and *Neocallimastix lanati* (S3) [10], to enhance the biodegradability of polyhydroxyalkanoate (PHA), cellulose acetate (CA), and polylactic acid (PLA) biodegradable bio-based plastics (BPs) under AD conditions. Here, we showed that pretreatment of PHA with *N. californiae* improved its biodegradability in anaerobic sludge relative to untreated PHA, and pretreatment of CA with *N. lanati* improved its biodegradability in anaerobic sludge relative to untreated CA. These findings expand the conditions under which these plastics can biodegrade and highlight their potential as organic waste feedstocks for biomethane production. Pretreatment of PLA with *N. lanati* did not affect its biodegradability, demonstrating that AGF pretreatments are polymer design-specific. Next-generation sequencing methods were used to investigate changes in the community structure and gene expression of the sludge microbiome, as well as the gene expression of AGF during the pretreatment phase. Altogether, these results demonstrate for the first time that AGF can be effectively applied to enhance the biodegradation of bioplastics in anaerobic digestion systems, thereby converting carbon from plastic waste into useful bioenergy.

Methods

Anaerobic sludge microbiome experimental design

BP biodegradation was assessed under the following experimental conditions: i) anaerobic sludge supplemented with a BP that had been pretreated with AGF (BP + AGF + AS), ii) anaerobic sludge supplemented with a BP that had been thermally pretreated (described below) and pretreated with AGF (tBP + AGF + AS), iii) anaerobic sludge supplemented with an untreated BP (BP + AS), iv) anaerobic sludge supplemented with a BP that had been thermally pretreated (tBP + AS), v) anaerobic sludge supplemented with a four-day-old culture of AGF that contained no BP (AGF + AS), and vi) unsupplemented anaerobic sludge (AS).

All BP degradation experiments were conducted in 80 mL serum bottles, each filled with 30 mL of liquid and sealed with air-tight butyl rubber stoppers. Anaerobic sludge was obtained from the AD reactor at the El Estero wastewater treatment plant (Santa Barbara, CA, USA). This sludge was stabilized by filtering it through a sieve, adding the filtered sludge to a 1 L bottle with a screw cap and rubber stopper, adding 30% volume of MC minus medium [22] and 3 g/L of cellulose (Sigma, 11363-250G), and incubating at 37°C for 3 days with regular degassing to prevent pressure buildup. Each serum bottle contained MC minus medium supplemented with 3 g/L of cellulose: 12 mL for bottles that would be inoculated with AGF (i.e. BP + AGF + AS, tBP + AGF + AS, and AGF + AS) and 15 mL for bottles that would not be inoculated with AGF (i.e.

BP + AS, tBP + AS, and AS). Thermal pretreatment of BPs (i.e. tBP + AGF + AS and tBP + AS) refers to incubation of the BPs in the MC minus medium at 70 °C for 1 hour prior to the four-day incubation (and prior to AGF inoculation for tBP + AGF + AS).

Two AGF species were used in this experiment: *Neocallimastix californiae* (G1) [14] and *Neocallimastix lanati* (S3) [10]. Based on preliminary experiments in which all three BPs were tested with both AGF (Fig. S1), we selected G1 to pretreat PHA and S3 to pretreat PLA and CA. For each of the three selected pairings, a preculture of the corresponding AGF was created by growing the fungus anaerobically in MC minus medium supplemented with 10 g/L of cellulose at 39°C for three days. Three mL of liquid (excluding fungal mat material) from this AGF preculture was transferred via sterile syringe needles to the bottles containing 12 mL of MC minus medium described above. All bottles were then incubated at 39°C for four days. On the fourth day, 15 mL of the stabilized anaerobic sludge was added, and the cultures were incubated at 39°C for an additional 56 days, following the ISO 13975:2019 standard [23].

Bioplastic material, preparation, pretreatment, and degradation

The following BPs were tested: PHA straw (Good Start Packaging; PHASTRAW-REG-BULK; 0.006 in thick), CA film (Sigma Aldrich; GF22418322-1EA; 0.05 mm thick), and PLA film (GF27769304-1EA; 0.025 mm thick). The BPs were cut into strips of 1 cm^2, weighed, disinfected with 80% ethanol for 1 hour, and then UV-sterilized for 30 minutes after the alcohol was removed with a sterile pipette. A total of 3 g/L of the sterilized BPs was added to the individual serum bottles containing 12-15 mL of MC minus medium with 3 g/L cellulose (i.e. BP + AGF + AS, tBP + AGF + AS, BP + AS, and tBP + AS) in an anaerobic chamber. tBP + AGF + AS and tBP + AS bottles were thermally pretreated at 70 °C for 1 hour and cooled at room temperature and on ice prior to AGF inoculation, while BP + AGF + AS and BP + AS bottles received no thermal pretreatment and were instead immediately inoculated with AGF. All bottles were incubated at 39 °C for four days before adding 15 mL of stabilized anaerobic sludge and incubating at 39 °C for 56 days, as described above.

After the 56-day incubation in anaerobic sludge, the extent of BP degradation was evaluated by comparing the initial weight (i.e. dry matter content) of the BP to that of the BP at the end of the experiment. To measure BP weight at the end of the experiment, the contents of the serum bottle were filtered through a 500 µm sieve. The BP debris was washed twice with water and incubated with 2% SDS for 2 hours under shaking to detach the microbial biofilm. Following this step, the debris was washed twice again with water and dried overnight at 40 °C before weighing. Individual BP pieces were separately collected for scanning electron microscopy (SEM) and Fourier transform infrared spectroscopy (FTIR) analysis and processed as described below.

Biogas and volatile fatty acids measurements

After the bottles were inoculated with anaerobic sludge, biogas production was regularly monitored by gas sampling through the septum. The CO_2 and CH_4 contents were measured using

potassium hydroxide replacement equipment, as specified in [24]. Monoculture samples for volatile fatty acid (VFA) analysis were collected on the fourth day of AGF pretreatment and stored at -20 °C. The VFA extraction protocol involved adding 50 µL of 50 mM H_2SO_4 to 500 µL of sample. Standards for acetate, formate, propionate, lactate, ethanol, and butyrate were prepared by spiking the chemicals into MC minus media at concentrations of 0.1 g/L and 1.0 g/L. To each standard, 50 µL of 50 mM H_2SO_4 was added to 500 µL of solution. Samples and standards were vortexed and centrifuged, and the resulting supernatant was filtered through a 0.22 µm syringe filter (Millex) into vial inserts for analysis. The VFA content was measured using high-performance liquid chromatography (HPLC; Agilent 1260 Infinity) equipped with an autosampler unit (1260 ALS) and an organic acids column (Bio-Rad Aminex HPX-87H). A 5 mM H_2SO_4 mobile phase was used at a flow rate of 0.6 mL/min, as previously described [25], with detection performed using a variable wavelength detector.

Sampling and extraction of macromolecules

To analyze the microbial composition and gene expression of the anaerobic sludge microbiome, the anaerobic sludge was sampled from each serum bottle using a sterile syringe and needle through the septum, immediately stabilized in liquid nitrogen, and stored at -80°C. DNA and RNA were co-extracted from the preserved sludge using the AllPrep PowerViral DNA/RNA Kit (Qiagen) following the manufacturer's protocol. After extraction, the eluent was divided into two aliquots: one that was treated with 1 µL of 10 µg/mL RNase A (Sigma) for 30 minutes at room temperature to isolate DNA, and one that was treated with TURBO DNase (Invitrogen) according to the manufacturer's protocol to isolate RNA. The quality and quantity of the extracted nucleic acids were evaluated using a 2200 TapeStation (Agilent) and Qubit 2.0 Fluorometer (Invitrogen), respectively. DNA and RNA extracts were stored at -20 °C and -80 °C, respectively, until library preparation was performed.

Microbiome library preparation, sequencing, and statistical analysis

Bacterial and archaeal 16S rRNA gene amplicon libraries were prepared following previously published protocols [26] and sequenced on the Illumina NextSeq2000 platform at the University of Luxembourg. In brief, modified versions of the universal primers S-D-Bact-0909-a-S-18 and S-Univ-1392-a-A-15 for bacteria, and S-D-Arch-0519-a-S-15 and S-D-Arch-1041-a-A-18 for archaea, were used in conjunction with the Nextera XT Index Kit V2 (Illumina) and Q5 Hot Start High-Fidelity 2× Master Mix (New England Biolabs). A two-step PCR protocol was employed to amplify fragments of approximately 484 bp (spanning the V6–V8 regions) for bacteria and 526 bp (spanning the V4–V6 regions) for archaea. Amplicon sequencing reads were processed with the ampliseq pipeline (v2.12.0) [27] for 39 bacterial and archaeal samples each. The pipeline implemented in nextflow [28] includes preprocessing with Cutadapt (v4.6) [29], quality filtering and ASV inference with DADA2 (v1.30.0) [30], and downstream analysis with qiime2 (v2023.7.0) [31] and phyloseq (v1.54.2) [32]. Taxonomic classification of ASVs was carried out against the Silva database nr99_v138.2 [33] with DADA2. Out of each set of 39 samples, 39

samples were retained for subsequent analysis for bacteria and 39 samples for archaea (Tables S2-S3).

For beta-diversity ordination and PERMANOVA analyses, ASV tables were rarefied to 3,000 reads per archaea sample and 10,000 reads per bacteria sample prior to Bray-Curtis distance calculation to control for uneven sequencing depth. The qiime2 output of the amplicon sequencing samples was imported into R (v4.5.0) using the qiime2R package and converted into a phyloseq object using the phyloseq package. Non-metric multidimensional scaling (NMDS) plots were created using the phyloseq package in R to visualize Bray-Curtis dissimilarity of the bacterial and archaeal communities across timepoints and experimental conditions. Two comparisons of relative abundances of bacteria and archaea were then evaluated: i) anaerobic sludge supplemented with CA that had been pretreated with *N. lanati* vs. anaerobic sludge supplemented with untreated CA (CA + S3 + AS vs. control CA + AS), and ii) anaerobic sludge supplemented with PHA that had been pretreated with *N. californiae* vs. anaerobic sludge supplemented with untreated PHA (PHA + G1 + AS vs. control PHA + AS). For this differential abundance analysis, ANCOM-BC2 (v2.13.2) [34] was applied to unrarefied count data, consistent with its built-in bias-correction framework for sampling depth (Tables S4-S7). Due to low sample sizes of the control CA + AS and control PHA + AS archaeal samples, these samples were combined when performing the comparisons of CA + S3 + AS vs. control CA + AS and PHA + G1 + AS vs. control PHA + AS. A heatmap of the differential abundances of bacteria and archaea with a Benjamini-Hochberg-adjusted p-value (q-value) < 0.05 was created using the pheatmap package in R. Metadata for all 16S samples is shown in Tables S8-S9.

The mRNA libraries (prokaryotic) were prepared using the Zymo-Seq RiboFree® Total RNA Library Kit (Zymo Research) following the manufacturer's protocol. Sequencing was performed on the NextSeq2000 platform (University of Luxembourg) using a P4 flow cell with a read length of 2 × 150 bp. Sequencing of 20 libraries yielded 430 Gb (on average 21 Gb per sample) of raw read data. Raw paired-end reads were pre-processed with IMP3 [35], a sample-wise integrated meta-omics analysis pipeline executed within Snakemake (v7.15.2) [36]. Quality trimming was performed with Trimmomatic (v0.39) [37], followed by removal of polyG and polyA stretches using Cutadapt (v3.4) [29]. Ribosomal RNA reads were removed with SortMeRNA [38]. Reads mapping to the fungal reference genomes Neolan1 [10] and Neosp1 [14] (retrieved from JGI MycoCosm [39]) were excluded from downstream analysis. After pre-processing, 51 Gb of bacterial and archaeal transcripts were retained across all samples. Overall, bacterial and archaeal read-counts were heavily reduced in the rRNA removal step (mean retention 11%), while 0.7% raw reads were mapped to fungal references and discarded for prokaryotic metatranscriptomics analysis.

Processed reads from all samples were co-assembled using MEGAHIT (v1.2.9) [40]. Open reading frames were predicted using a modified version of Prokka (v1.14.6) [41] incorporating Prodigal (v2.6.3) [42] with an option to call partial genes. Functional annotation was performed using eggnog-mapper (v2.1.9) [43] with the eggNOG 5.0 database, and CAZymes were

annotated using dbCAN (v4.1.4) with the database version 13 [44]. Reads were mapped back to the co-assembly with bowtie2 (v2.5.4) [45] and quantified on the level of predicted coding sequences with featureCounts [46] with the -s 2 parameter. Taxonomic annotation of assembled transcripts (contig-level) was carried out with mmseqs2 [47] easy-taxonomy workflow vs the NR and GTDB databases.

To analyze the differential transcriptional abundances of COG categories in the metatranscriptomic data, gene-level counts belonging to each COG category were added together. MaAsLin2 (v1.24.1) [48] was then used to compare transcriptional abundances for counts aggregated by COG category for i) CA + S3 + AS vs. control CA + AS and ii) PHA + G1 + AS vs. control PHA + AS (Table S10). This analysis was repeated for Kyoto Encyclopedia of Genes and Genomes (KEGG) modules (Table S11) and CAZyme families (Table S12). Heatmaps of the differential transcriptional abundances of clusters of orthologous genes (COGs) and KEGG modules were created using the pheatmap package in R. Volcano plots of the resulting MaAsLin2 coefficients and q-values were created using the ggplot2 package (v4.0.3) [49] in R to identify the most significantly enriched CAZyme families in the anaerobic sludge microbiome. Additionally, CAZyme classes (GH, PL, CE, AA, GT, CBM) were extracted from dbCAN annotations. Read counts were normalized to relative abundance within each sample, then averaged across biological replicates for each phylum-CAZyme class pairing. Only the ten most abundant phyla (by total relative abundance) were retained, with all remaining phyla collapsed into an “Others” category. Chord diagrams depicting the relative contribution of each phylum to each CAZyme class were generated in R using the circlize package (v0.4.18) [50]. Metadata for the metatranscriptomic samples is shown in Table S13, and taxa and counts for each CAZyme category by condition are shown in Table S14.

Scanning electron microscopy

The PHA, CA, and PLA BPs were visualized using SEM for the following conditions: untreated BPs, BPs after four days of AGF pretreatment, untreated BPs after 56 days in anaerobic sludge, and BPs after four days of AGF pretreatment and 56 days in anaerobic sludge. The BPs were washed twice by gently soaking them in water and then incubated overnight at 4°C in 2% glutaraldehyde/phosphate buffer. Following this step, the bioplastic films were washed with water and sequentially dehydrated in ethanol solutions of 50%, 75%, 90%, and 100%, each for 10 minutes. The BPs were then air-dried and stored at room temperature in sealed Petri dishes. The dried, dehydrated BP materials were mounted on aluminum stubs using adhesive copper tape and sputter coated with an ultra-thin layer of gold to improve conductivity. Observation and imaging of the samples were performed using an Apreo C scanning electron microscope (Thermo Fisher Scientific) with a 5 kV accelerating voltage, 0.4 nA beam current, and 10 mm nominal working distance.

Fourier transform infrared spectroscopy

BPs were placed on a sample plate, and the IR spectrum was recorded in the range of 4000–500 cm^{-1} wavenumbers, with 2-3 replicates for each sample, using a Bruker IFS 66v FTIR spectrometer (Bruker Optik GmbH, Ettlingen, Germany). Untreated BP controls were also analyzed. Assessment of the tCA film was not possible at the end of the experiment due to extensive degradation and/or the inability to recover large enough film pieces from the sample. The spectral data were recorded as % transmittance and analyzed by constructing and subtracting a baseline to correct for baseline variations. Subsequently, the spectra were normalized to observe variations in the peak intensities of the characteristic peaks in the FTIR spectra.

Monoculture transcriptomic experimental design, library preparation, sequencing, and statistical analysis

After the anaerobic sludge experiment (described above) was completed, a second experiment was performed to compare i) the biogas production of *N. lanati* grown with CA (CA + S3) to that of *N. lanati* grown without CA (S3) and ii) the biogas production of *N. californiae* grown with PHA (PHA + G1) to that of *N. californiae* grown without PHA (G1) during the AGF pretreatment phase. Like the first experiment, this experiment was conducted in 80 mL serum bottles, each filled with 12 mL of MC minus medium [22] supplemented with 3 g/L of cellulose and sealed with air-tight butyl rubber stoppers. Experimental conditions included i) medium supplemented with a BP and AGF (BP + AGF), ii) medium supplemented with AGF only (AGF), and iii) unsupplemented media (Media). A preculture of the corresponding AGF was created by growing the fungus in MC minus medium supplemented with 10 g/L of cellulose for 3 days at 39°C. Three mL of liquid from this AGF preculture was used to inoculate the 12 mL of MC minus medium, and all bottles were then incubated at 39°C until biogas pressure, which was measured to track AGF growth throughout the experiment, plateaued. On the fourth day, 5 of the 8 biological replicates from each condition with AGF (i.e. CA + S3, S3, PHA + G1, and G1) were harvested for RNA extraction. An equal volume of in-house prepared RNAlater solution [51] was added to each harvested bottle, and the mixtures were then poured into 50 mL conical tubes. These tubes were centrifuged at 4 °C and 12,000 × g for 15 minutes. The mixtures were decanted, and the fungal pellets were then flash frozen in liquid nitrogen and stored at -80 °C. RNA was extracted from these pellets using the Qiagen RNeasy Mini Kit, following the "Purification of Total RNA from Plant Cells and Tissues and Filamentous Fungi" protocol from the RNeasy Mini Handbook. The "Optional On-Column DNase Digestion with the RNase-Free DNase Set" protocol was followed during these extractions to remove DNA, and the final RNA product was eluted in 50 µL of RNase-free water. The quality and quantity of these RNA extracts were evaluated using a 2200 TapeStation (Agilent Technologies, Palo Alto, CA, USA) and an Invitrogen Qubit 2.0 Fluorometer (ThermoFisher Scientific, Waltham, MA, USA), respectively.

The CA + S3 and S3 RNA samples were shipped to Azenta Life Sciences (South Plainfield, NJ, USA) for strand-specific RNA sequencing. Read quality was evaluated using fastqc and raw

reads were trimmed using fastp (v1.0.1) with default parameters [52]. The filtered reads were aligned to the reference *N. lanati* genome [10,39] using HISAT2 (v2.2.1) [53] and the resulting files were sorted and indexed using SAMtools (v1.7) [54]. Raw gene-level counts were then generated with featureCounts (v1.5.2; settings: -s 2 -p --primary options) [46]. Differential gene expression analysis was performed using this raw gene-level count matrix and DESeq2 (v1.40.2) [55] to compare the gene expression of the CA + S3 samples to that of the S3 samples (Table S15). The raw gene counts were converted into transcripts per million (TPM) counts for post-DESeq2 filtering. Before running DESeq2, genes with 0 raw counts across all CA + S3 and S3 samples were removed. After running DESeq2, only genes with an average TPM > 2 across all replicates for at least one condition were used for creating the heatmap in Figure 7. To create the heatmap, a cutoff of the absolute value of the $\log_2$ fold change (abs(LFC)) > 3 and the q-value < 0.01 was applied to the TPM-filtered DESeq2 output. Additionally, dbCAN3 (v3.0.7) [56] was used to identify the CAZyme genes in the *N. lanati* genome using default parameters. A gene was considered a CAZyme gene if it was annotated as such by at least 2 tools.

Of the filtered results, genes that were functionally annotated by the Joint Genome Institute's (JGI) annotation pipeline [57] and identified as CAZyme genes by dbCAN3 were selected to create the heatmap using the pheatmap package in R. The remaining unannotated genes that passed these filters were structurally annotated using AlphaFold and Foldseek. Structures of these 67 proteins were predicted using Alphafold 3 [58], which was performed on California NanoSystems Institute's high performance computing clusters; parallel computing was implemented to predict multiple proteins at one time. The proteins that were larger in size (>3000 kDa) were predicted using the webserver (https://alphafoldserver.com/welcome). The highest ranked structure prediction from AlphaFold for each protein was used for further analysis. The per-residue local distance difference test (pLDDT) confidence scores for the protein structure models were retrieved from the B-factor field. Structural homology searches for annotation were carried out using Foldseek [59]. Annotations that had an e-value of < 1e-04 and probability of 1.00 were considered (Table S16). Metadata for the transcriptomic samples is shown in Table S17. Genes upregulated in this transcriptomic dataset were matched to genes identified by Wilken et al. [10] (available in "cazyreport.txt" at https://github.com/stelmo/iNlan20/tree/main/OmicsData/Cazymes) and by Lawson et al. [60] (available in their Supplementary Material as Supplementary Table 3, "media-3.csv") (Table S18).

Results

Two strains of AGF, *N. californiae* (G1) and *N. lanati* (S3), were assessed in this study for their capacity as fungal pretreatments to improve the biodegradation of CA, PHA, and PLA BPs under anaerobic digestion conditions. To evaluate the impact of AGF pretreatments on these different BPs, we assessed biodegradation of each BP that was pretreated with both AGF (Fig. S1). Based on these preliminary results, three AGF-BP pairings were selected for this study: PHA pretreated by *N. californiae* (G1-PHA), CA pretreated by *N. lanati* (S3-CA), and PLA pretreated by *N.*

lanati (S3-PLA). Each AGF was first grown in monoculture in MC minus medium supplemented with cellulose and its paired BP for four days, which is referred to as the AGF pretreatment. For each BP, some samples were thermally pretreated before the AGF pretreatment to further improve the BP biodegradability. After the AGF pretreatment, anaerobic sludge was added to the culture and incubated for an additional 56 days, according to the ISO 13975:2019 standard [23] (Fig. 1).

Pretreatment of PHA and CA with AGF increased biogas production from anaerobic sludge

Cumulative biogas production from the anaerobic sludge culture was measured throughout the 56-day incubation to compare the extent of biodegradation of the AGF-pretreated BPs to that of the untreated BP controls (Fig. 2). Sludge supplemented with *N. californiae*-pretreated PHA (PHA + G1 + AS) produced 72.9% more biogas than sludge supplemented with an untreated PHA control (PHA + AS), 92.0% more biogas than sludge supplemented with an *N. californiae* control grown for four days without PHA (G1 + AS), and 69.1% more biogas than an unsupplemented sludge control (AS) (Fig. 2A-B). Similarly, sludge supplemented with thermally and *N. californiae*-pretreated PHA (tPHA + G1 + AS) produced 57.0% more biogas than sludge supplemented with a thermally pretreated PHA control (tPHA + AS), 79.1% more than control G1 + AS, and 57.8% more than control AS (Fig. 2A-B). Each of these comparisons was determined to be statistically significant ($p < 0.05$) via Welch's t-test.

Likewise, sludge supplemented with *N. lanati*-pretreated CA (CA + S3 + AS) produced 39.0% more biogas than sludge supplemented with an untreated CA control (CA + AS), 65.0% more biogas than sludge supplemented with an *N. lanati* control grown for four days without CA (S3 + AS), and 86.2% more biogas than control AS (Fig. 2C-D). Sludge supplemented with thermally and *N. lanati*-pretreated CA (tCA + S3 + AS) produced 73.8% more biogas than sludge supplemented with a thermally pretreated CA control (tCA + AS), 75.9% more biogas than control S3 + AS, and 98.5% more biogas than control AS (Fig. 2C-D). Again, each of these comparisons was determined to be statistically significant.

In contrast, sludge supplemented with *N. lanati*-pretreated PLA (PLA + S3 + AS) and sludge supplemented with thermally and *N. lanati*-pretreated PLA (tPLA + S3 + AS) both produced much less biogas than the G1-PHA and S3-CA pairings. PLA + S3 + AS produced 31.9% more biogas than sludge supplemented with an untreated PLA control (PLA + AS), 10.0% more than control S3 + AS, and 24.2% more than control AS (Fig. 2E-F). tPLA + S3 + AS produced 45.7% more biogas than sludge supplemented with a thermally pretreated PLA control (tPLA + AS), 11.2% more biogas than control S3 + AS, and 25.6% more biogas than control AS (Fig. 2E-F). However, the comparisons of i) PLA + S3 + AS to control S3 + AS and ii) tPLA + S3 + AS to control S3 + AS were determined to be non-significant. These observations suggest that the success of an AGF pretreatment in enhancing BP biodegradability in anaerobic sludge is therefore specific to the AGF-BP pairing.

To confirm that CH_4 can be produced during these biological processes, the CH_4 content of the biogas produced by the anaerobic sludge was measured during the sludge incubation stage corresponding to the maximum biogas productivity (i.e. 21-32 days). Average CH_4 content of sludge biogas was the highest for both CA + S3 + AS (64.0 ± 0.9%) and tCA + S3 + AS (64.1 ± 5.6%) and was the lowest among the AGF-pretreated BPs for PLA + S3 + AS (55.3 ± 2.8%) (Table S1). Additionally, HPLC analysis of these samples during the AGF pretreatment phase showed that metabolite production by both AGF with and without their paired BPs was consistent except for tCA + S3, which produced higher levels of succinate, lactate, and ethanol in comparison to the other conditions (Fig. S2).

BP surface analysis indicated AGF-induced BP damage and degradation

SEM was used to assess the ability of the AGF to induce damage to the surface of the BPs. This was done under the following conditions: i) untreated BP control, ii) BP after four days of AGF pretreatment, iii) untreated BP control after 56 days of incubation in anaerobic sludge, and iv) BP after four days of AGF pretreatment and 56 days of incubation in anaerobic sludge (Fig. 3A). Based on SEM visualization during the AGF pretreatment, *N. californiae* extensively colonized PHA and *N. lanati* extensively colonized CA, while *N. lanati* only slightly colonized PLA. By the end of the 56-day incubation in anaerobic sludge, the surface of the *N. californiae*-pretreated PHA was rougher and more pitted in comparison to the untreated PHA control. Likewise, the *N. lanati*-pretreated CA had been sheared into many layers, while the untreated CA control had remained rather intact. In contrast, both the *N. lanati*-pretreated PLA and the untreated PLA control remained intact and undamaged by the end of the 56-day sludge incubation. These observations demonstrate that substantial fungal colonization during the AGF pretreatment phase was followed by enhanced BP degradation reflected in the biogas measurements described above, while minimal fungal colonization was followed by poor BP degradation.

BP biodegradation was further evaluated by comparing the weights of the BPs that were extracted from the anaerobic sludge at the end of their 56-day incubation to their initial weights. tCA + S3 + AS and CA + S3 + AS samples experienced the most weight loss, followed by PHA + G1 + AS and tPHA + G1 + AS samples, whereas PLA + S3 + AS and tPLA + S3 + AS samples experienced the least weight loss, thus corroborating the findings of the biogas measurements (Fig. 3B).

FTIR was also used to characterize the BP surfaces under these conditions. The spectra showed differences in the degradation behavior among the treated samples. In comparison to the untreated PHA control, the treated PHA samples showed a progressive decrease in the intensity of the carbonyl peaks around 1722 cm^{-1}, indicating possible cleavage of the ester bonds. Additionally, an increase in the intensity of the hydroxyl region (3700 – 2900 cm^{-1}) for some samples suggests the formation of hydroxyl-containing degradation products. The PHA samples treated with the consortium of G1 + AS cultures at 60 days experienced pronounced spectral changes consistent with notable polymer chain breakdown (Fig. S3). In contrast, CA showed less

evidence of extensive degradation among all treated samples. In comparison to the untreated CA control, a minor increase in carbonyl intensity at 1731 cm^{-1} was observed, and this could suggest deacetylation rather than polymer chain breakdown (Fig. S4). Furthermore, PLA samples showed a similar trend to CA. A moderate increase in carbonyl intensities compared to the untreated PLA control was also observed. This increase also suggests hydrolysis of the ester bond rather than extensive polymer degradation (Fig. S5). The increase is less observed for sample PLA + S3 Day 4 and PLA + S3 + AS Day 60, showing that the treatment with the other consortium showed promising results.

AGF-pretreated CA and PHA induced significant taxa shifts in the anaerobic sludge microbiome

Based on the observations from biogas (Fig. 2), SEM (Fig. 3A), weight loss (Fig. 3B), and FTIR (Fig. S3-S5) measurements, only the CA + S3 + AS, control CA + AS, PHA + G1 + AS, and control PHA + AS samples were selected for further 16S rRNA gene amplicon sequencing and metatranscriptomic analyses of the anaerobic sludge microbiome. PLA samples were excluded from further analysis, as PLA biodegradation was non-significant under these experimental conditions. To characterize bacteria and archaea in the anaerobic sludge that were enriched by the AGF-pretreated BPs, DNA was harvested from CA + S3 + AS, control CA + AS, PHA + G1 + AS, and control PHA + AS samples collected at four timepoints during the 56-day incubation: 21 days (t1), 27 days (t2), 31 days (t3), and 47 days (t4). 16S rRNA gene amplicon sequencing was then applied to these samples (Fig. 4). A NMDS plot of this data shows that the archaeal and bacterial communities of the anaerobic sludge supplemented with the AGF-pretreated BPs developed differently than those of the anaerobic sludge supplemented with the untreated BP controls (Fig. 4A-B). Archaeal community composition differed significantly between the CA + S3 + AS and control CA + AS groups (PERMANOVA, Bray-Curtis, $R^2 = 0.284$, $p = 0.012$) and between the PHA + G1 + AS and control PHA + AS groups (PERMANOVA, Bray-Curtis, $R^2 = 0.473$, $p = 0.009$). Bacterial community composition also differed significantly between the CA + S3 + AS and control CA + AS groups (PERMANOVA, Bray-Curtis, $R^2 = 0.272$, $p = 0.001$) and between the PHA + G1 + AS and control PHA + AS groups (PERMANOVA, Bray-Curtis, $R^2 = 0.263$, $p = 0.005$) [61].

Comparison of CA + S3 + AS and control CA + AS groups over all timepoints revealed that *Methanosarcina*, *Aminobacterium*, *Lachnospiraceae NK4A136 group*, *Lachnospiraceae AC2044 group*, *Oscillibacter*, *S50 wastewater-sludge group*, *AUTHM297*, and *Clostridium* were significantly enriched ($q < 0.05$), while *HN-HF0106* and *Victivallis* were significantly depleted. In contrast, comparison of PHA + G1 + AS and control PHA + AS groups revealed that *Methanosarcina*, *AUTHM297*, and *Clostridium* were significantly enriched, while *Saccharofermentans* were significantly depleted (Fig. 4C, Tables S2-S7). Together, these results show that the AGF-pretreated CA and AGF-pretreated PHA both induced taxonomic shifts within the anaerobic sludge microbiome, with each BP associated with a distinct set of enriched taxa.

AGF-pretreated CA and PHA induced significant changes in the gene expression of the anaerobic sludge microbiome

To compare the metatranscriptomic profiles of the anaerobic sludge microbiome in response to AGF-pretreated CA and PHA, samples were collected at t1 and t2 during the 56-day sludge incubation from the following conditions: CA + S3 + AS, control CA + AS, PHA + G1 + AS, and control PHA + AS. RNA was extracted from these samples and sequenced for metatranscriptomic analysis of prokaryotic transcripts. A multidimensional scaling (MDS) plot of this RNA-sequencing data showed that the control CA + AS samples and the control PHA + AS samples clustered together regardless of timepoint, indicating that gene expression of the sludge microbiome under these conditions was similar between substrates and remained stable across the two timepoints. Samples with AGF-pretreatment (CA + S3 + AS and PHA + G1 + AS) formed separate clusters from each other and the respective control samples, indicating distinct metatranscriptomic profiles. Additionally, PHA + G1 + AS expression profiles could be distinguished according to timepoint, reflecting changing gene expression patterns of that microbial community over time (Fig. S6).

The AGF-pretreated CA and PHA may have induced changes in gene expression and, by extension, the putative metabolic activity of the anaerobic sludge microbiome. The transcriptional abundances of COGs [62,63] in the anaerobic sludge supplemented with the AGF-pretreated BPs were compared to those in the anaerobic sludge supplemented with the untreated BP controls (Fig. 5A, Table S10). Transcripts belonging to COG categories D (Cell cycle control, cell division, chromosome partitioning), Z (Cytoskeleton), and C (Energy production and conversion) were significantly enriched in the CA + S3 + AS group relative to the control CA + AS group. Likewise, transcripts belonging to COG categories B (Chromatin structure and dynamics), J (Translation, ribosomal structure and biogenesis), and I (Lipid transport and metabolism) were significantly enriched in the PHA + G1 + AS group relative to the control PHA + AS group. Interestingly, transcripts belonging to COG categories N (cell motility), T (signal transduction), and W (extracellular structures) were significantly depleted in both AGF-treated BP conditions (CA + S3 + AS and PHA + G1 + AS) relative to their respective untreated controls, suggesting a coordinated adaptive response of the microbial community. This pattern could reflect a transition from an exploratory and environmentally responsive mode, characterized by active motility, environmental sensing, and surface colonization, toward a metabolically committed, energy-conserving state focused on substrate degradation.

While COG categories define broad functions, KEGG modules [64,65] resolve genes into specific pathways, offering finer insight into the metabolic processes potentially driving degradation of these AGF-pretreated BPs. To examine these processes, the transcriptional abundances of KEGG modules in the anaerobic sludge supplemented with the AGF-pretreated BPs were compared to those in the anaerobic sludge supplemented with the untreated BP controls (Fig. 5B). The comparison of CA + S3 + AS to control CA + AS revealed that several modules associated with carbohydrate metabolism and acetate utilization were enriched in the

CA + S3 + AS group relative to the control. These included core glycolytic modules M00001 (Glycolysis, Embden-Meyerhof pathway, glucose => pyruvate) and M00002 (Glycolysis, core module involving three-carbon compounds), as well as M00003 (Gluconeogenesis, oxaloacetate => fructose-6P). In contrast, the comparison of PHA + G1 + AS to control PHA + AS revealed that more general modules associated with anabolic metabolism (M00580 - Pentose phosphate pathway, M00049 - Adenine ribonucleotide biosynthesis, M00016/M00525/M00526 - Lysine biosynthesis) were enriched in the PHA + G1 + AS group relative to the control. To further probe this community's response and determine how the *N. californiae*-pretreated PHA altered the anaerobic sludge microbiome across the two timepoints, PHA + G1 + AS at t2 was compared to PHA + G1 + AS at t1. This comparison revealed the enrichment of fatty acid metabolism pathways, including M00087 (β-oxidation) and M00113 (Jasmonic acid biosynthesis), as well as sugar acid catabolism pathways that feed into central carbon metabolism, including M00061 (D-Glucuronate degradation, D-glucuronate => pyruvate + D-glyceraldehyde-3P) and M00631 (D-Galacturonate degradation (bacteria), D-galacturonate => pyruvate + D-glyceraldehyde-3P). Together, these modules indicate a shift toward carbohydrate metabolism in the anaerobic sludge supplemented with *N. lanati*-pretreated CA and toward fatty acid metabolism over time in the anaerobic sludge supplemented with *N. californiae*-pretreated PHA. Additionally, the comparison of CA + S3 + AS to control CA + AS showed that M00378 (F420 biosynthesis, archaea) was enriched in the CA + S3 + AS group relative to the control, while the comparison of PHA + G1 + AS to control PHA + AS showed that M00836 (Coenzyme F430 biosynthesis, sirohydrochlorin => coenzyme F430) was enriched in the PHA + G1 + AS group relative to the control. Both of these modules are indicators of methanogenesis activity in the anaerobic sludge [66,67], aligning with the findings of the CH_4 content measurements and the enrichment of methanogens seen in the 16S analysis.

Given that AGF-pretreated BPs, especially the *N. lanati*-pretreated CA, showed enriched carbohydrate metabolism activity within the anaerobic sludge, CAZyme expression was also evaluated. Like the previous analysis of COGs and KEGG modules, transcriptional abundances of CAZyme families in the anaerobic sludge supplemented with the AGF-pretreated BPs were compared to those in the sludge supplemented with the untreated BP controls (Fig. 6A-B). The comparison of CA + S3 + AS to control CA + AS revealed that acetylesterases (CE12) from *UBA1723*, *Fibrobacter*, *Mitsuaria*, *Ruminiclostridium*, *Pelomonas*, *JAGNGI01*, and *LD21*; endoglucanases (GH45) from *Fibrobacter*; and cellulose binding modules (CBM6) from *UBA1723*, *Ruminiclostridium*, *JAGNGI01*, *RGIG10190*, *Pelomonas*, *Hungateiclostridium*, and *MWFF01* were enriched in the CA + S3 + AS group relative to the control (Fig. 6A, Table S14). Glycosyltransferases involved in general polysaccharide biosynthesis (GT1 and GT119) were also enriched. Likewise, the comparison of PHA + G1 + AS to control PHA + AS revealed that diverse polysaccharide degraders (GH16, GH23, GH66, GH130, CE4, and GT35), and polysaccharide binders and synthesizers (CBM13, GT2, GT3, GT4, and GT66) were enriched in the PHA + G1 + AS group relative to the control (Fig. 6B). The top 10 phyla contributing to CAZyme expression in CA + S3 + AS were Thermotogota, Pseudomonadota, Halobacteriota,

Fibrobacterota, Desulfobacterota, Chloroflexota, Bacteroidota, Bacillota B, and Bacillota A (Fig. 6C), with Fibrobacterota and Bacillota B replacing Verrucomicrobiota and Atribacterota in CA + AS (Fig. 6D). The top 10 phyla contributing to CAZyme expression in PHA + G1 + AS were Thermotogota, Pseudomonadota, Halobacteriota, Desulfobacterota, Chloroflexota, Bacteroidota, Bacillota B, Bacillota A, and Atribacterota (Fig. 6E), with Bacillota B replacing Verrucomicrobiota in PHA + AS (Figure 6F).

N. lanati *can partially metabolize CA, but* N. californiae *cannot metabolize PHA*

To assess AGF–BP interactions during the AGF pretreatment phase, *N. lanati* and *N. californiae* were each grown in monoculture with and without their respective BP. Biogas production was significantly higher from *N. lanati* grown with CA than from *N. lanati* grown without it, whereas the presence of PHA did not impact biogas production from *N. californiae* (Fig. 7A-B). Based on these observations, only the *N. lanati* samples grown with and without CA were selected for further transcriptomic analysis.

In accordance with the growth pattern of AGF [68], RNA sequencing was performed on RNA that was extracted on the fourth day from these *N. lanati* monocultures. Differential expression analysis revealed that *N. lanati* strongly upregulated many CAZymes, especially GHs and CBMs, in the presence of CA (Fig. 7C, Table S15). In fact, 9 of the 10 most strongly upregulated genes (ranked by adjusted p-value) were GHs and CBMs (Fig. S7). Upregulated CAZymes included CE1, GH3, GH5, GH10, GH6, and CBM13 families, in addition to several other CAZyme families. Furthermore, AlphaFold and Foldseek were used to perform structural analysis and search on the upregulated genes that were annotated as hypothetical protein genes. These tools identified genes encoding glycoside hydrolases, feruloyl esterases, xylanases, and MAM domain-containing proteins that were strongly upregulated by *N. lanati* in the presence of CA and are also included in Figure 7C (Table S17).

Discussion

Anaerobic digestion is a robust biological system that converts organic waste into renewable biogas and nutrient-rich digestate, facilitating significant reductions in greenhouse gas emissions and enabling circular economy waste management [69]. This makes anaerobic digestion environmentally and economically advantageous over composting at large scale; however, it is generally less efficient at degrading certain organic substrates in comparison to composting [70]. PHA plastics, particularly polyhydroxybutyrate, have been found to degrade efficiently under anaerobic digestion conditions; however, PLA and CA plastics, in addition to several other common plastics, have exhibited poor biodegradability in these systems, making them unsuitable feedstocks [71]. Therefore, recalcitrant substrates like plastics require a form of pretreatment to improve their biodegradability under anaerobic digestion conditions.

Anaerobic gut fungi enhance CA and PHA biodegradability through different mechanisms

Anaerobic gut fungi have previously been shown to improve biogas production, CH_4 composition, and organic waste decomposition in anaerobic digesters [72]. However, their potential to improve the degradation of synthetic plastics, especially under anaerobic digestion conditions, has not yet been explored. In this study, we demonstrated that *N. lanati* enhanced CA biodegradation and *N. californiae* enhanced PHA biodegradation in anaerobic digester sludge, whereas *N. lanati* had no significant effect on PLA biodegradation (Fig. 2). SEM images further illustrated that the extensive colonization of CA and PHA by AGF was followed by considerable surface damage after incubation in the anaerobic sludge, while PLA was colonized to a lesser extent by AGF and remained undamaged by the end of incubation (Fig. 3). Fungal hyphae are known to physically penetrate polymer surface defects, applying mechanical forces that propagate further damage to the material that can enhance or be enhanced by concurrent enzymatic degradation [73,74]. The extensive colonization of PHA and CA by AGF damaged the BP surfaces, thus making them more amenable to further damage and biodegradation by the microbes in the anaerobic sludge.

Although both the *N. lanati*-pretreated CA and *N. californiae*-pretreated PHA were rendered more biodegradable in the anaerobic sludge, only *N. lanati* could partially metabolize its paired substrate (CA) in monoculture during the AGF pretreatment phase, whereas *N. californiae* could not metabolize PHA (Fig. 7A-B), suggesting that AGF enhance BP degradation through different mechanisms. Cellulose acetate degradation mainly involves deacetylation by esterases and depolymerization by cellulases [75–78]. The deacetylation step is typically the rate-determining step in the degradation of cellulose acetate. It releases acetic acid and regenerates the underlying cellulose backbone, which is then hydrolyzed by cellulases. The differential gene expression analysis revealed that *N. lanati* upregulated many CAZymes, including CE1, GH3, GH5, GH10, and GH6 families (Fig. 7C). CE1 is a functionally diverse CAZyme family that includes both acetyl xylan esterases and feruloyl esterases and has been characterized from several thermophilic fungal species [79]. Additionally, GH3 (β-glucosidase), GH5 (endoglucanase), GH6 (cellobiohydrolase), and GH10 (xylanase) families have previously been shown to work together to achieve efficient hydrolysis of pretreated corn stover [80]. The coordinated expression of secreted acetyl xylan esterases and glycoside hydrolase activities is therefore consistent with the established two-step mechanism of cellulose acetate biodegradation. Additionally, many of the upregulated CAZyme genes belong to the CBM13 family, which is known to enhance catalytic efficiency by anchoring its associated glycoside hydrolase domain to carbohydrate substrates [81,82]. These CEs, GHs, and CBMs may therefore work together to degrade the complex CA substrate.

Notably, the CAZymes expressed by *N. lanati* when grown on synthetic CA during the AGF pretreatment phase have also been reported to be expressed by *N. lanati* grown on natural lignocellulose. 285 of the CAZymes significantly upregulated in our RNA-sequencing data were shown in a previous study to be expressed by *N. lanati* in rumen-derived enriched consortia grown on sorghum [60] (Table S18). Another study identified 271 genes in the *N. lanati* genome

that encode GHs containing dockerin domains, which are thought to be incorporated into cellulosomal complexes [10]. Our study showed that 108 of these dockerin domain-containing GH genes were significantly upregulated by *N. lanati* when grown on CA, suggesting that *N. lanati*'s plant-adapted cellulosomal machinery can also be mobilized against certain synthetic plastics like CA (Table S18). Further functional characterization of these cellulosome-associated GH enzymes will clarify their role in AGF-mediated bioplastic degradation.

In addition to these CAZymes, several genes encoding proteins that lacked sequence-based annotation were also upregulated by *N. lanati*. Extended re-annotation with Foldseek resolved the putative function of several proteins that lacked sequence-based annotation. These included an α/β-hydrolase carbohydrate esterase that Foldseek identified as a feruloyl esterase, which may act on the acetyl esters of CA in addition to the CE1 family, as fold-based annotation cannot resolve acetyl- from feruloyl-ester specificity and the substrate contains no ferulate/lignin. Additionally, genes encoding proteins with β-sandwich adhesion-type folds that Foldseek identified as MAM domains were upregulated. As the metazoan receptor-signaling contexts of these folds are absent in anaerobic fungi, these can be interpreted as extracellular adhesion/interaction modules whose induction may reflect the requirement to anchor the fungus and its secreted enzyme complexes to the hydrophobic CA substrate [83]. Altogether, while both AGF colonized their respective BP during the AGF pretreatment phase and thus contributed to mechanical hydrolysis of the BPs, only *N. lanati* acted as a further enzymatic pretreatment on CA. Both of these mechanisms damaged the BP surface during their AGF pretreatment, thus rendering the materials more susceptible to biodegradation by the microbial communities in the anaerobic sludge. These results thus illustrate the different ways that AGF can enhance the biodegradability of BPs in anaerobic sludge.

AGF-pretreated BPs enriched several biomass- and polymer-degrading taxa in the anaerobic sludge microbiome

Both the *N. lanati*-pretreated CA and *N. californiae*-pretreated PHA induced significant changes in the composition of the anaerobic sludge microbial community. For instance, *Methanosarcina*, which were strongly enriched in both comparisons of CA + S3 + AS to control CA + AS and PHA + G1 + AS to control PHA + AS, are known to consume acetate, H_2/CO_2, methanol, and methylamines, acting at the terminal step of biodegradation processes [84]. *Methanosarcina barkeri* have been shown to consume acetate produced from cellulose fermentation by a coculture of a cellulose-degrading anaerobic fungus and a hydrogen-consuming *Methanobrevibacter* sp. [85]. The triculture of these three microbes improved the extent of cellulose degradation in comparison to that of the anaerobic fungus monoculture or either fungus-methanogen coculture, highlighting the important role each species played in enhancing biomass metabolism. Additionally, several genera of bacteria that are associated with the degradation of plant carbohydrates were significantly enriched in the CA + S3 + AS group relative to the control CA + AS group, including *Lachnospiraceae NK4A136 group* [86], *Lachnospiraceae AC2044 group* [87], and *AUTHM297* [88]. Likewise*, AUTHM297* and

Clostridium were significantly enriched in the PHA + G1 + AS group relative to the control PHA + AS group and are associated with the degradation of organic matter and cellulose [88–90]. Notably, *Clostridium* spp., in addition to being strong lignocellulose degraders, have been reported to be involved in the degradation of different kinds of PHAs [91,92]. These findings suggest that strong cellulose degraders were enriched by the *N. lanati*-pretreated CA, whereas strong carbohydrate degraders and recognized PHA degraders were enriched by the *N. californiae*-pretreated PHA, highlighting the different and BP-specific community-level responses induced by the BPs in the sludge microbiome.

AGF-pretreated BPs showed enrichment of distinct CAZymes and metabolic pathways in the anaerobic sludge microbiome

Furthermore, both the *N. lanati*-pretreated CA and the *N. californiae*-pretreated PHA induced significant substrate-specific changes in the gene expression of the anaerobic sludge microbiome. The CBM6, CE12, and GH45 CAZyme families enriched in the CA + S3 + AS group relative to the control CA + AS group depict a mechanism enabling the degradation of the CA backbone [93,94]. CBM6s bind to carbohydrate substrates to anchor their attached enzyme to a carbohydrate surface and enhance its ability to break down the substrate. CE12s (acetyl esterases) remove acetyl groups from polysaccharides, enabling the deacetylation of CA, and GH45s (endoglucanases) then hydrolyze the resulting cellulose backbone. The GT1 and GT119 CAZyme families also enriched in this comparison likely reflect biosynthesis and growth within the microbial community in response to the increase of sugars from this hydrolysis. Furthermore, Fibrobacterota, a phylum encompassing many well-known and robust cellulose-degraders [95–98], became one of the top 10 phyla contributing CAZymes in the CA + S3 + AS samples, further suggesting that cellulolytic behavior increased in the CA + S3 + AS group relative to the control CA + AS group. This is also reflected in the enrichment of COG C (Energy production and conversion) and glycolytic KEGG modules in this comparison, which indicate that the microbial community was actively metabolizing the CA-derived products for energy production.

Unlike the *N. lanati*-pretreated CA, the degradation of the *N. californiae*-pretreated PHA was unlikely to have been driven by CAZymes. When PHA is in contact with natural microbial systems, its ester bonds can be hydrolyzed by PHA depolymerases, generating smaller units, mainly D-3-hydroxybutyrate and acetoacetate [99]. Under anaerobic conditions, these monomers or oligomers are taken up and enter the β-oxidation pathway in anaerobic bacteria [99]. Some lipases are also capable of degrading PHAs [100–102]. Whereas CA resembles the cellulose found in natural biomass, PHA better resembles lipids because it is a polyester of hydroxyacids, which are similar to fatty acids. It therefore requires metabolic pathways targeted at lipids rather than carbohydrates, which is reflected in the enrichment of COG I (Lipid transport and metabolism), as well as the β-oxidation and jasmonic acid synthesis [103] KEGG modules, in the PHA + G1 + AS group relative to the control PHA + AS group. Collectively, these observations suggest that *N. lanati*-pretreated CA and *N. californiae*-pretreated PHA elicited fundamentally different enzymatic responses within the anaerobic sludge microbiome to achieve biodegradation

of these substrates. This evidence of BP-specific responses in the enzymatic profile of the anaerobic sludge microbiome supports the findings of BP-specific taxonomic enrichments in the sludge from the 16S analysis and highlights key pathways driving the metabolism of these plastics.

An improved control for identifying the effects of AGF-pretreated BPs on the anaerobic sludge microbiome could be anaerobic sludge supplemented with an untreated BP that was added to a four-day-old AGF culture. This would eliminate the effects of AGF-derived metabolites and AGF biomass on the anaerobic sludge community, as the presence of AGF changed the metabolite profile of the media that the anaerobic sludge was added to (Fig. S2). However, because the metabolite profiles were similar for both *N. lanati* and *N. californiae* regardless of BP presence, metabolic changes in the anaerobic sludge that were driven by differences in the AGF-inoculated media would have been the same for the CA + S3 + AS vs. control CA + AS and PHA + G1 + AS vs. control PHA + AS comparisons. Instead, the observed changes in the taxonomic and gene expression profiles of the anaerobic sludge microbiome were specific to the supplemented BP substrate, suggesting that these changes were driven by BP degradation rather than metabolite differences in the media. Furthermore, these differences in metabolite profiles between the AGF + BP + AS and control BP + AS samples did not impact biogas production from the anaerobic sludge. This suggests that, while BP degradation measurably perturbed the anaerobic sludge system, the metabolite differences themselves did not.

Conclusions

Anaerobic gut fungi are powerful organisms that have great potential as enzymatic or mechanical pretreatments on certain plastic designs to improve their biodegradability under anaerobic digestion conditions, enabling these substrates to be used as organic waste feedstocks to produce economically useful products such as CH_4. These biological pretreatments do not fully degrade the plastic material, but rather damage it enough to unlock the plastic-specific degradative machinery within the anaerobic sludge microbiome. This work advances the design of biological waste-treatment systems aimed at converting diverse plastic waste streams into renewable energy. The CAZyme families and carbohydrate metabolism modules enriched during *N. lanati*-pretreated CA degradation, along with the fatty acid metabolism modules enriched during *N. californiae*-pretreated PHA degradation, represent promising engineering targets for improving BP degradation efficiency in anaerobic digesters. Similarly, the dockerin-containing GH genes upregulated by *N. lanati* during its pretreatment of CA offer additional targets for engineering AGF-based pretreatment strategies for synthetic plastics. With the development of more bio-based plastics that are derived from plant material, these pretreatment-enhanced biological systems can contribute to a circular carbon economy that reduces plastic waste and limits the emission of greenhouse gases into the atmosphere.

List of abbreviations

BP: Bio-based biodegradable plastic

AD: Anaerobic digestion

AGF: Anaerobic gut fungi

PHA: Polyhydroxyalkanoate

CA: Cellulose acetate

PHA + G1 + AS: Anaerobic sludge supplemented with *N. californiae*-pretreated PHA

tPHA + G1 + AS: Anaerobic sludge supplemented with thermally and *N. californiae*-pretreated PHA

PHA + AS: Anaerobic sludge supplemented with untreated PHA

tPHA + AS: Anaerobic sludge supplemented with thermally pretreated PHA

G1 + AS: Anaerobic sludge supplemented with *N. californiae* grown for four days without PHA

CA + S3 + AS: Anaerobic sludge supplemented with *N. lanati*-pretreated CA

tCA + S3 + AS: Anaerobic sludge supplemented with thermally and *N. lanati*-pretreated CA

CA + AS: Anaerobic sludge supplemented with untreated CA

tCA + AS: Anaerobic sludge supplemented with thermally pretreated CA

PLA + S3 + AS: Anaerobic sludge supplemented with *N. lanati*-pretreated PLA

tPLA + S3 + AS: Anaerobic sludge supplemented with thermally and *N. lanati*-pretreated PLA

PLA + AS: Anaerobic sludge supplemented with untreated PLA

tPLA + AS: Anaerobic sludge supplemented with thermally pretreated PLA

S3 + AS: Anaerobic sludge supplemented with *N. lanati* grown for four days without CA or PLA

AS: Unsupplemented anaerobic sludge

COG: Clusters of Orthologous Genes

KEGG: Kyoto Encyclopedia of Genes and Genomes

GH: Glycoside hydrolase

PL: Polysaccharide lyase

CE: Carbohydrate esterase

AA: Auxiliary activities

GT: Glycosyltransferase

CBM: Carbohydrate-binding module

Declarations

Ethics approval and consent to participate

Not applicable.

Consent for publication

Not applicable.

Availability of data and material

The raw reads for total RNA sequencing, 16S amplicon sequencing, and isolate RNAseq have been deposited in the NCBI SRA under the bioproject accession number PRJNA1489402. The datasets generated and/or analyzed during the current study are available in the AGF_BP_pretreatment GitHub repository, available at https://github.com/colleenahern/BPs_AGF_pretreatment.

Competing interests

The authors declare that they have no competing interests.

Funding

A portion of this work was funded by the Office of Biological and Environmental Research of the U.S. Department of Energy via DE-SC0022142 and also via the Joint BioEnergy Institute (JBEI, https://ror.org/03ww55028) through contract DE-AC02–05CH11231. MC was supported by the Luxembourg National Research Fund (NTER/MOBILITY/2022-2/SR/17563365/FungiPlast and FNR, INTER/FORMAS/22/501100001866-17467995/BIOHOLISTIC grants).

Authors' contributions

The microbiome study was designed by MC and the isolate study was designed by MC and CBA. MC performed biogas, HPLC, and FTIR measurements; extracted DNA and RNA; and performed library preparation and sequencing for the anaerobic sludge experiment. CBA performed biogas measurements, extracted RNA, and performed sequencing for the monoculture experiment. CBA performed bioinformatics and statistical analyses, wrote the manuscript, and designed figures. MH performed metatranscriptomic assembly and 16S sequencing data processing. RR performed Alphafold and Foldseek analyses and provided interpretations to data

generated. HMP performed SEM measurements. IEI performed FTIR analysis and provided interpretations to data generated. SJ, BZ, and EMB aided in creating the AGF cultures used in these experiments. MAO and MC supervised the study, provided training, and reviewed all data. All authors read and approved the final manuscript.

Acknowledgments

The authors acknowledge the use of the Biological Nanostructures Laboratory within the California NanoSystems Institute, supported by the University of California, Santa Barbara and the University of California, Office of the President. Use was made of computational facilities purchased with funds from the National Science Foundation (CNS-1725797) and administered by the Center for Scientific Computing (CSC). The CSC is supported by the California NanoSystems Institute and the Materials Research Science and Engineering Center (MRSEC; NSF DMR 2308708) at UC Santa Barbara. The microbiome sequencing experiments presented in this paper were carried out at the LCSB sequencing platform (RRID: SCR_021931) at the University of Luxembourg.

Authors' information

Department of Chemical Engineering, University of California, Santa Barbara, CA, 93106, USA
Colleen B. Ahern, Shirley Jin, Ramya Ragunathan, Hugh M. Purdy, Bo Zhang, Elaina M. Blair, Michelle A. O'Malley & Magdalena Calusinska

Luxembourg Institute of Science and Technology, Luxembourg
Malte Herold, Iikpoemugh Elo Imiete, Magdalena Calusinska

Joint BioEnergy Institute (JBEI), Emeryville, CA, 94608, USA
Michelle A. O'Malley

Department of Bioengineering, University of California, Santa Barbara, CA, 93106, USA
Michelle A. O'Malley

References

1. Global Plastics Outlook: Economic Drivers, Environmental Impacts and Policy Options. Paris: OECD Publishing; 2022. https://doi.org/10.1787/de747aef-en

2. Leejarkpai T, Suwanmanee U, Rudeekit Y, Mungcharoen T. Biodegradable kinetics of plastics under controlled composting conditions. Waste Management. 2011;31:1153–61. https://doi.org/10.1016/j.wasman.2010.12.011

3. Bhatt AH, Tao L. Economic perspectives of biogas production via anaerobic digestion. Bioengineering. MDPI AG; 2020;7:1–19. https://doi.org/10.3390/bioengineering7030074

4. Abraham A, Park H, Choi O, Sang BI. Anaerobic co-digestion of bioplastics as a sustainable mode of waste management with improved energy production – A review. Bioresour Technol. 2021;322. https://doi.org/10.1016/j.biortech.2020.124537

5. Jin Y, Cai F, Song C, Liu G, Chen C. Degradation of biodegradable plastics by anaerobic digestion: Morphological, micro-structural changes and microbial community dynamics. Science of the Total Environment. Elsevier B.V.; 2022;834. https://doi.org/10.1016/j.scitotenv.2022.155167

6. Quecholac-Piña X, Hernández-Berriel MDC, Mañón-Salas MDC, Espinosa-Valdemar RM, Vázquez-Morillas A. Degradation of plastics under anaerobic conditions: A short review. Polymers (Basel). MDPI AG; 2020;12:1–18. https://doi.org/10.3390/polym12010109

7. Mat Yasin N, Akkermans S, Van Impe JFM. Enhancing the biodegradation of (bio)plastic through pretreatments: A critical review. Waste Management. Elsevier Ltd; 2022;150:1–12. https://doi.org/10.1016/j.wasman.2022.06.004

8. Srikanth M, Sandeep TSRS, Sucharitha K, Godi S. Biodegradation of plastic polymers by fungi: a brief review. Bioresour Bioprocess. Springer Science and Business Media Deutschland GmbH; 2022;9. https://doi.org/10.1186/s40643-022-00532-4

9. Solomon K V, Haitjema CH, Henske JK, Gilmore SP, Borges-Rivera D, Lipzen A, et al. Early-branching gut fungi possess a large, comprehensive array of biomass-degrading enzymes. Science (1979) [Internet]. 2016;351. https://doi.org/10.1126/science.aad1431

10. Wilken SE, Monk JM, Leggieri PA, Lawson CE, Lankiewicz TS, Seppälä S, et al. Experimentally Validated Reconstruction and Analysis of a Genome-Scale Metabolic Model of an Anaerobic Neocallimastigomycota Fungus. mSystems [Internet]. 2021;6. https://doi.org/10.1126/science.aad1431

11. Cantarel BI, Coutinho PM, Rancurel C, Bernard T, Lombard V, Henrissat B. The Carbohydrate-Active EnZymes database (CAZy): An expert resource for glycogenomics. Nucleic Acids Res. 2009;37. https://doi.org/10.1093/nar/gkn663

12. Levasseur A, Drula E, Lombard V, Coutinho PM, Henrissat B. Expansion of the enzymatic repertoire of the CAZy database to integrate auxiliary redox enzymes. Biotechnol Biofuels. 2013;6. https://doi.org/10.1186/1754-6834-6-41

13. Lankiewicz TS, Lillington SP, O'Malley MA. Enzyme Discovery in Anaerobic Fungi (Neocallimastigomycetes) Enables Lignocellulosic Biorefinery Innovation. Microbiology and Molecular Biology Reviews. American Society for Microbiology; 2022;86. https://doi.org/10.1128/mmbr.00041-22

14. Haitjema CH, Gilmore SP, Henske JK, Solomon K V., De Groot R, Kuo A, et al. A parts list for fungal cellulosomes revealed by comparative genomics. Nat Microbiol. Nature Publishing Group; 2017;2. https://doi.org/10.1038/nmicrobiol.2017.87

15. Gruninger RJ, Puniya AK, Callaghan TM, Edwards JE, Youssef N, Dagar SS, et al. Anaerobic fungi (phylum Neocallimastigomycota): Advances in understanding their taxonomy, life cycle, ecology, role and biotechnological potential. FEMS Microbiol Ecol. Blackwell Publishing Ltd; 2014;90:1–17. https://doi.org/10.1111/1574-6941.12383

16. Lillington SP, Chrisler W, Haitjema CH, Gilmore SP, Smallwood CR, Shutthanandan V, et al. Cellulosome localization patterns vary across life stages of anaerobic fungi. mBio. American Society for Microbiology; 2021;12. https://doi.org/10.1128/mBio.00832-21

17. Brown JL, Gierke T, Butkovich L V., Swift CL, Singan V, Daum C, et al. High-quality RNA extraction and the regulation of genes encoding cellulosomes are correlated with growth stage in anaerobic fungi. Frontiers in Fungal Biology. Frontiers Media SA; 2023;4. https://doi.org/10.3389/ffunb.2023.1171100

18. Lankiewicz TS, Choudhary H, Gao Y, Amer B, Lillington SP, Leggieri PA, et al. Lignin deconstruction by anaerobic fungi. Nat Microbiol. Nature Research; 2023;8:596–610. https://doi.org/10.1038/s41564-023-01336-8

19. Koller M, Heeney D, Mukherjee A. Biodegradability of polyhydroxyalkanoate (PHA) biopolyesters in nature: a review. Biodegradation. Springer Science and Business Media B.V.; 2025. https://doi.org/10.1007/s10532-025-10164-y

20. Gadaleta G, De Gisi S, Chong ZK, Heerenklage J, Notarnicola M, Kuchta K, et al. Degradation of thermoplastic cellulose acetate-based bioplastics by full-scale experimentation of industrial anaerobic digestion and composting. Chemical Engineering Journal. Elsevier B.V.; 2023;462. https://doi.org/10.1016/j.cej.2023.142301

21. Kang JH, Kang SW, Kim WJ, Kim DH, Im SW. Anaerobic Co-Digestion of Bioplastics and Food Waste under Mesophilic and Thermophilic Conditions: Synergistic Effect and Biodegradation. Fermentation. MDPI; 2022;8. https://doi.org/10.3390/fermentation8110638

22. Bo Z, Ivan H, Jan T, Yuqian G, M WS, M FJ, et al. The anaerobic fungus Caecomyces churrovis produces H2 via a non-bifurcating NADH-dependent enzyme complex. mBio [Internet]. American Society for Microbiology; 2026;0:e01643-26. https://doi.org/10.1128/mbio.01643-26

23. ISO 13975:2019 Plastics — Determination of the ultimate anaerobic biodegradation of plastic materials in controlled slurry digestion systems — Method by measurement of biogas production [Internet]. https://www.iso.org/standard/74992.html

24. Hiligsmann S, Masset J, Hamilton C, Beckers L, Thonart P. Comparative study of biological hydrogen production by pure strains and consortia of facultative and strict anaerobic bacteria. Bioresour Technol. 2011;102:3810–8. https://doi.org/10.1016/j.biortech.2010.11.094

25. Peng X, Wilken SE, Lankiewicz TS, Gilmore SP, Brown JL, Henske JK, et al. Genomic and functional analyses of fungal and bacterial consortia that enable lignocellulose breakdown in goat gut microbiomes. Nat Microbiol. Nature Research; 2021;6:499–511. https://doi.org/10.1038/s41564-020-00861-0

26. Calusinska M, Goux X, Fossépré M, Muller EEL, Wilmes P, Delfosse P. A year of monitoring 20 mesophilic full-scale bioreactors reveals the existence of stable but different core microbiomes in bio-waste and wastewater anaerobic digestion systems. Biotechnol Biofuels. BioMed Central Ltd.; 2018;11. https://doi.org/10.1186/s13068-018-1195-8

27. Straub D, Blackwell N, Langarica-Fuentes A, Peltzer A, Nahnsen S, Kleindienst S. Interpretations of Environmental Microbial Community Studies Are Biased by the Selected 16S rRNA (Gene) Amplicon Sequencing Pipeline. Front Microbiol. Frontiers Media S.A.; 2020;11. https://doi.org/10.3389/fmicb.2020.550420

28. Di Tommaso P, Chatzou M, Floden EW, Barja PP, Palumbo E, Notredame C. Nextflow enables reproducible computational workflows. Nat Biotechnol [Internet]. 2017;35:316–9. https://doi.org/10.1038/nbt.3820

29. Martin M. Cutadapt removes adapter sequences from high-throughput sequencing reads. EMBnet J [Internet]. 2011;17:10–2. https://api.semanticscholar.org/CorpusID:84784389

30. Callahan BJ, McMurdie PJ, Rosen MJ, Han AW, Johnson AJA, Holmes SP. DADA2: High-resolution sample inference from Illumina amplicon data. Nat Methods. Nature Publishing Group; 2016;13:581–3. https://doi.org/10.1038/nmeth.3869

31. Bolyen E, Rideout JR, Dillon MR, Bokulich NA, Abnet CC, Al-Ghalith GA, et al. Reproducible, interactive, scalable and extensible microbiome data science using QIIME 2. Nat Biotechnol [Internet]. 2019;37:852–7. https://doi.org/10.1038/s41587-019-0209-9

32. McMurdie PJ, Holmes S. phyloseq: An R Package for Reproducible Interactive Analysis and Graphics of Microbiome Census Data. PLoS One [Internet]. Public Library of Science; 2013;8:e61217-. https://doi.org/10.1371/journal.pone.0061217

33. Quast C, Pruesse E, Yilmaz P, Gerken J, Schweer T, Yarza P, et al. The SILVA ribosomal RNA gene database project: improved data processing and web-based tools. Nucleic Acids Res [Internet]. 2013;41:D590–6. https://doi.org/10.1093/nar/gks1219

34. Lin H, Peddada S Das. Multigroup analysis of compositions of microbiomes with covariate adjustments and repeated measures. Nat Methods. Nature Research; 2024;21:83–91. https://doi.org/10.1038/s41592-023-02092-7

35. Narayanasamy S, Jarosz Y, Muller EEL, Heintz-Buschart A, Herold M, Kaysen A, et al. IMP: a pipeline for reproducible reference-independent integrated metagenomic and metatranscriptomic analyses. Genome Biol [Internet]. 2016;17:260. https://doi.org/10.1186/s13059-016-1116-8

36. Köster J, Rahmann S. Snakemake—a scalable bioinformatics workflow engine. Bioinformatics [Internet]. 2012;28:2520–2. https://doi.org/10.1093/bioinformatics/bts480

37. Bolger AM, Lohse M, Usadel B. Trimmomatic: a flexible trimmer for Illumina sequence data. Bioinformatics [Internet]. 2014;30:2114–20. https://doi.org/10.1093/bioinformatics/btu170

38. Kopylova E, Noé L, Touzet H. SortMeRNA: fast and accurate filtering of ribosomal RNAs in metatranscriptomic data. Bioinformatics [Internet]. 2012;28:3211–7. https://doi.org/10.1093/bioinformatics/bts611

39. Grigoriev I V, Nikitin R, Haridas S, Kuo A, Ohm R, Otillar R, et al. MycoCosm portal: gearing up for 1000 fungal genomes. Nucleic Acids Res [Internet]. 2014;42:D699–704. https://doi.org/10.1093/nar/gkt1183

40. Li D, Liu C-M, Luo R, Sadakane K, Lam T-W. MEGAHIT: an ultra-fast single-node solution for large and complex metagenomics assembly via succinct de Bruijn graph. Bioinformatics [Internet]. 2015;31:1674–6. https://doi.org/10.1093/bioinformatics/btv033

41. Seemann T. Prokka: rapid prokaryotic genome annotation. Bioinformatics [Internet]. 2014;30:2068–9. https://doi.org/10.1093/bioinformatics/btu153

42. Hyatt D, Chen G-L, LoCascio PF, Land ML, Larimer FW, Hauser LJ. Prodigal: prokaryotic gene recognition and translation initiation site identification. BMC Bioinformatics [Internet]. 2010;11:119. https://doi.org/10.1186/1471-2105-11-119

43. Cantalapiedra CP, Hernández-Plaza A, Letunic I, Bork P, Huerta-Cepas J. eggNOG-mapper v2: Functional Annotation, Orthology Assignments, and Domain Prediction at the Metagenomic Scale. bioRxiv [Internet]. 2021;2021.06.03.446934. https://doi.org/10.1101/2021.06.03.446934

44. Yin Y, Mao X, Yang J, Chen X, Mao F, Xu Y. dbCAN: a web resource for automated carbohydrate-active enzyme annotation. Nucleic Acids Res [Internet]. 2012;40:W445–51. https://doi.org/10.1093/nar/gks479

45. Langmead B, Salzberg SL. Fast gapped-read alignment with Bowtie 2. Nat Methods [Internet]. 2012;9:357–9. https://doi.org/10.1038/nmeth.1923

46. Liao Y, Smyth GK, Shi W. FeatureCounts: An efficient general purpose program for assigning sequence reads to genomic features. Bioinformatics. Oxford University Press; 2014;30:923–30. https://doi.org/10.1093/bioinformatics/btt656

47. Mirdita M, Steinegger M, Breitwieser F, Söding J, Levy Karin E. Fast and sensitive taxonomic assignment to metagenomic contigs. Bioinformatics [Internet]. 2021;37:3029–31. https://doi.org/10.1093/bioinformatics/btab184

48. Mallick H, Rahnavard A, McIver LJ, Ma S, Zhang Y, Nguyen LH, et al. Multivariable association discovery in population-scale meta-omics studies. PLoS Comput Biol. Public Library of Science; 2021;17. https://doi.org/10.1371/journal.pcbi.1009442

49. Hadley Wickham. ggplot2: Elegant Graphics for Data Analysis [Internet]. Springer-Verlag New York; 2016 [cited 2026 Aug 10]. https://ggplot2.tidyverse.org. Accessed 10 Aug 2026

50. Gu Z, Gu L, Eils R, Schlesner M, Brors B. circlize implements and enhances circular visualization in R. Bioinformatics [Internet]. 2014;30:2811–2. https://doi.org/10.1093/bioinformatics/btu393

51. Malmstrom R. RNAlater Recipe. protocols.io. 2015; https://doi.org/dx.doi.org/10.17504/protocols.io.c56y9d

52. Chen S, Zhou Y, Chen Y, Gu J. Fastp: An ultra-fast all-in-one FASTQ preprocessor. Bioinformatics. Oxford University Press; 2018. p. i884–90. https://doi.org/10.1093/bioinformatics/bty560

53. Kim D, Langmead B, Salzberg SL. HISAT: A fast spliced aligner with low memory requirements. Nat Methods. Nature Publishing Group; 2015;12:357–60. https://doi.org/10.1038/nmeth.3317

54. Li H, Handsaker B, Wysoker A, Fennell T, Ruan J, Homer N, et al. The Sequence Alignment/Map format and SAMtools. Bioinformatics. 2009;25:2078–9. https://doi.org/10.1093/bioinformatics/btp352

55. Love MI, Huber W, Anders S. Moderated estimation of fold change and dispersion for RNA-seq data with DESeq2. Genome Biol. BioMed Central Ltd.; 2014;15. https://doi.org/10.1186/s13059-014-0550-8

56. Zheng J, Ge Q, Yan Y, Zhang X, Huang L, Yin Y. DbCAN3: Automated carbohydrate-Active enzyme and substrate annotation. Nucleic Acids Res. Oxford University Press; 2023;51:W115–21. https://doi.org/10.1093/nar/gkad328

57. Huntemann M, Ivanova NN, Mavromatis K, Tripp HJ, Paez-Espino D, Tennessen K, et al. The standard operating procedure of the DOE-JGI Metagenome Annotation Pipeline (MAP v.4). Stand Genomic Sci. BioMed Central Ltd.; 2016;11. https://doi.org/10.1186/s40793-016-0138-x

58. Abramson J, Adler J, Dunger J, Evans R, Green T, Pritzel A, et al. Accurate structure prediction of biomolecular interactions with AlphaFold 3. Nature. Nature Research; 2024;630:493–500. https://doi.org/10.1038/s41586-024-07487-w

59. van Kempen M, Kim SS, Tumescheit C, Mirdita M, Lee J, Gilchrist CLM, et al. Fast and accurate protein structure search with Foldseek. Nat Biotechnol. Nature Research; 2024;42:243–6. https://doi.org/10.1038/s41587-023-01773-0

60. Lawson CE, Howard JP, Lankiewicz TS, Brown JB, Singer SW, Garcia Martin H, et al. CAZyme domain architectures suggest fine-scale functional differentiation among anaerobic fungi and bacteria during lignocellulose conversion to volatile fatty acids. bioRxiv [Internet]. Cold Spring Harbor Laboratory; 2026; https://doi.org/10.64898/2026.02.09.704939

61. Anderson MJ. A new method for non-parametric multivariate analysis of variance. Austral Ecol [Internet]. John Wiley & Sons, Ltd; 2001;26:32–46. https://doi.org/https://doi.org/10.1111/j.1442-9993.2001.01070.pp.x

62. Tatusov RL, Galperin MY, Natale DA, Koonin E V. The COG database: a tool for genome-scale analysis of protein functions and evolution [Internet]. Nucleic Acids Res. 2000. http://www.ncbi.nlm.nih.gov/COG

63. Galperin MY, Wolf YI, Makarova KS, Alvarez RV, Landsman D, Koonin E V. COG database update: Focus on microbial diversity, model organisms, and widespread pathogens. Nucleic Acids Res. Oxford University Press; 2021;49:D274–81. https://doi.org/10.1093/nar/gkaa1018

64. Kanehisa M, Goto S. KEGG: Kyoto Encyclopedia of Genes and Genomes [Internet]. Nucleic Acids Res. 2000. http://www.genome.ad.jp/kegg/

65. Kanehisa M, Furumichi M, Tanabe M, Sato Y, Morishima K. KEGG: New perspectives on genomes, pathways, diseases and drugs. Nucleic Acids Res. Oxford University Press; 2017;45:D353–61. https://doi.org/10.1093/nar/gkw1092

66. Chris G, Hafna AF, Elaaf MA, M LB, Gunjan P, C WA, et al. Physiology, Biochemistry, and Applications of F420- and Fo-Dependent Redox Reactions. Microbiology and Molecular Biology Reviews [Internet]. American Society for Microbiology; 2016;80:451–93. https://doi.org/10.1128/mmbr.00070-15

67. Moore SJ, Sowa ST, Schuchardt C, Deery E, Lawrence AD, Ramos JV, et al. Elucidation of the biosynthesis of the methane catalyst coenzyme F430. Nature [Internet]. 2017;543:78–82. https://doi.org/10.1038/nature21427

68. Butkovich L V., Leggieri PA, Lillington SP, Navaratna TA, Swift CL, Malinov NG, et al. Separation of life stages within anaerobic fungi (Neocallimastigomycota) highlights differences in global transcription and metabolism. Fungal Genetics and Biology. Academic Press Inc.; 2025;176. https://doi.org/10.1016/j.fgb.2024.103958

69. Huang X. The Promotion of Anaerobic Digestion Technology Upgrades in Waste Stream Treatment Plants for Circular Economy in the Context of “Dual Carbon”: Global Status,

Development Trend, and Future Challenges. Water (Basel) [Internet]. 2024;16. https://doi.org/10.3390/w16243718

70. Lin L, Xu F, Ge X, Li Y. Improving the sustainability of organic waste management practices in the food-energy-water nexus: A comparative review of anaerobic digestion and composting. Renewable and Sustainable Energy Reviews [Internet]. 2018;89:151–67. https://doi.org/https://doi.org/10.1016/j.rser.2018.03.025

71. Mashhadi B, Mostafa A, Calabrò PS, Dhar BR. Biodegradable or bottleneck? A critical review of anaerobic digestion of bioplastics. Waste Dispos Sustain Energy [Internet]. 2026;8:233–48. https://doi.org/10.1007/s42768-025-00265-y

72. Yıldırım E, Ince O, Aydin S, Ince B. Improvement of biogas potential of anaerobic digesters using rumen fungi. Renew Energy [Internet]. 2017;109:346–53. https://doi.org/https://doi.org/10.1016/j.renene.2017.03.021

73. Okal EJ, Heng G, Magige EA, Khan S, Wu S, Ge Z, et al. Insights into the mechanisms involved in the fungal degradation of plastics. Ecotoxicol Environ Saf [Internet]. 2023;262:115202. https://doi.org/https://doi.org/10.1016/j.ecoenv.2023.115202

74. Sánchez C. Fungal potential for the degradation of petroleum-based polymers: An overview of macro- and microplastics biodegradation. Biotechnol Adv [Internet]. 2020;40:107501. https://doi.org/https://doi.org/10.1016/j.biotechadv.2019.107501

75. Ishigaki T, Sugano W, Ike M, Fujita M. Enzymatic degradation of cellulose acetate plastic by Novel degrading bacterium Bacillus sp. S2055. J Biosci Bioeng [Internet]. 2000;90:400–5. https://doi.org/https://doi.org/10.1016/S1389-1723(01)80008-6

76. MORIYOSHI K, KOMA D, YAMANAKA H, SAKAI K, OHMOTO T. Expression and Characterization of a Thermostable Acetylxylan Esterase from Caldanaerobacter subterraneus subsp. tengcongensis Involved in the Degradation of Insoluble Cellulose Acetate. Biosci Biotechnol Biochem [Internet]. 2013;77:2495–8. https://doi.org/10.1271/bbb.130568

77. MORIYOSHI K, OHMOTO T, OHE T, SAKAI K. Purification and Characterization of an Esterase Involved in Cellulose Acetate Degradation by Neisseria sicca SB. Biosci Biotechnol Biochem [Internet]. 1999;63:1708–13. https://doi.org/10.1271/bbb.63.1708

78. Haske-Cornelius O, Pellis A, Tegl G, Wurz S, Saake B, Ludwig R, et al. Enzymatic Systems for Cellulose Acetate Degradation. Catalysts [Internet]. 2017;7. https://doi.org/10.3390/catal7100287

79. Dilokpimol A, Verkerk B, Li X, Bellemare A, Lavallee M, Frommhagen M, et al. Screening of novel fungal Carbohydrate Esterase family 1 enzymes identifies three novel dual feruloyl/acetyl xylan esterases. FEBS Lett [Internet]. John Wiley & Sons, Ltd; 2022;596:1932–43. https://doi.org/https://doi.org/10.1002/1873-3468.14322

80. Inoue H, Decker SR, Taylor LE, Yano S, Sawayama S. Identification and characterization of core cellulolytic enzymes from Talaromyces cellulolyticus (formerly Acremonium cellulolyticus) critical for hydrolysis of lignocellulosic biomass. Biotechnol Biofuels [Internet]. 2014;7:151. https://doi.org/10.1186/s13068-014-0151-5

81. FUJIMOTO Z. Structure and Function of Carbohydrate-Binding Module Families 13 and 42 of Glycoside Hydrolases, Comprising a β-Trefoil Fold. Biosci Biotechnol Biochem [Internet]. Taylor & Francis; 2013;77:1363–71. https://doi.org/10.1271/bbb.130183

82. Huang Y, Liu L, Wang R, Jiang T, Yu Q, Wang E, et al. Functional identification of carbohydrate-binding module 13 and its application to quantification of hemicellulose in gramineous plants. Int J Biol Macromol [Internet]. 2024;282:136752. https://doi.org/https://doi.org/10.1016/j.ijbiomac.2024.136752

83. Cismasiu VB, Denes SA, Reiländer H, Michel H, Szedlacsek SE. The MAM (Meprin/A5-protein/PTPmu) Domain Is a Homophilic Binding Site Promoting the Lateral Dimerization of Receptor-like Protein-tyrosine Phosphatase μ. Journal of Biological Chemistry [Internet]. Elsevier; 2004;279:26922–31. https://doi.org/10.1074/jbc.M313115200

84. Lackner N, Hintersonnleitner A, Wagner AO, Illmer P. Hydrogenotrophic methanogenesis and autotrophic growth of methanosarcina thermophila. Archaea. Hindawi Limited; 2018;2018. https://doi.org/10.1155/2018/4712608

85. Mountfort DO, Asher RA, Bauchop T. Fermentation of Cellulose to Methane and Carbon Dioxide by a Rumen Anaerobic Fungus in a Triculture with Methanobrevibacter sp. Strain RAl and Methanosarcina barkeri [Internet]. Appl. Environ. Microbiol. 1982. https://journals.asm.org/journal/aem

86. Lu S, Williams BA, Flanagan BM, Yao H, Mikkelsen D, Gidley MJ. Fermentation outcomes of wheat cell wall related polysaccharides are driven by substrate effects as well as initial faecal inoculum. Food Hydrocoll. Elsevier B.V.; 2021;120. https://doi.org/10.1016/j.foodhyd.2021.106978

87. Rabee AE, Abou-souliman I, Yousif AI, Lamara M, El-Sherbieny MA, Elwakeel EA, et al. Variations in rumen microbiota and host genome impacted feed efficiency in goat breeds. Front Microbiol. Frontiers Media SA; 2025;16. https://doi.org/10.3389/fmicb.2025.1492742

88. Rocha DHD, Sakamoto IK, Varesche MBA. Optimization of methane production from co-digestion of citrus agro-industrial waste in a two-stage system: Investigation of the effects of organic matter concentration and alkalinization. J Clean Prod. Elsevier Ltd; 2023;433. https://doi.org/10.1016/j.jclepro.2023.139793

89. Schwarz WH. The cellulosome and cellulose degradation by anaerobic bacteria. Appl. Microbiol. Biotechnol. 2001. p. 634–49. https://doi.org/10.1007/s002530100710

90. Deng W, Li C, Huang Y, Liu C, Li R, Li T, et al. Lignocellulose degradation capabilities and distribution of antibiotic resistance genes and virulence factors in Clostridium from the gut of giant pandas. Commun Biol. Nature Research; 2025;8. https://doi.org/10.1038/s42003-025-08943-7

91. Derkenne P, Chatellard L, Béline F, Pierson-Wickmann AC, Gontard N, Dabert P. Understanding the biodegradation of PHBV/Cellulose composites in mesophilic anaerobic digestion. Science of the Total Environment. Elsevier B.V.; 2025;959. https://doi.org/10.1016/j.scitotenv.2024.178224

92. Sun J, Zhou T, Yin F, Wang S. Anaerobic co-biodegradation of polyhydroxyalkanoate and swine manure for volatile fatty acid production: The impact of C/N ratios and microbial dynamics. Bioresour Technol. Elsevier Ltd; 2025;418. https://doi.org/10.1016/j.biortech.2024.131995

93. Carbohydrate Active Enzymes database [Internet]. http://www.cazy.org/. [cited 2026 May 19]. http://www.cazy.org/. Accessed 19 May 2026

94. Drula E, Garron ML, Dogan S, Lombard V, Henrissat B, Terrapon N. The carbohydrate-active enzyme database: Functions and literature. Nucleic Acids Res. Oxford University Press; 2022;50:D571–7. https://doi.org/10.1093/nar/gkab1045

95. Ransom-Jones E, Jones DL, McCarthy AJ, McDonald JE. The Fibrobacteres: An Important Phylum of Cellulose-Degrading Bacteria. Microb. Ecol. 2012. p. 267–81. https://doi.org/10.1007/s00248-011-9998-1

96. Raut MP, Couto N, Karunakaran E, Biggs CA, Wright PC. Deciphering the unique cellulose degradation mechanism of the ruminal bacterium Fibrobacter succinogenes S85. Sci Rep. Nature Publishing Group; 2019;9. https://doi.org/10.1038/s41598-019-52675-8

97. Xie X, Yang C, Guan LL, Wang J, Xue M, Liu JX. Persistence of cellulolytic bacteria fibrobacter and treponema after short-term corn stover-based dietary intervention reveals the potential to improve rumen fibrolytic function. Front Microbiol. Frontiers Media S.A.; 2018;9. https://doi.org/10.3389/fmicb.2018.01363

98. Kobayashi Y, Shinkai T, Koike S. Ecological and physiological characterization shows that Fibrobacter succinogenes is important in rumen fiber digestion — Review. Folia Microbiol (Praha) [Internet]. 2008;53:195–200. https://doi.org/10.1007/s12223-008-0024-z

99. Paloyan A, Tadevosyan MM, Ghevondyan D, Khoyetsyan L, Karapetyan M, Margaryan A, et al. Biodegradation of polyhydroxyalkanoates: current state and future prospects. Front Microbiol [Internet]. 2025;Volume 16-2025. https://doi.org/10.3389/fmicb.2025.1542468

100. Jaeger KE, Steinbüchel A, Jendrossek D. Substrate specificities of bacterial polyhydroxyalkanoate depolymerases and lipases: bacterial lipases hydrolyze poly(omega-

hydroxyalkanoates). Appl Environ Microbiol [Internet]. American Society for Microbiology; 1995;61:3113–8. https://doi.org/10.1128/aem.61.8.3113-3118.1995

101. Tokiwa Y, Calabia BP. Review Degradation of microbial polyesters. Biotechnol Lett [Internet]. 2004;26:1181–9. https://doi.org/10.1023/B:BILE.0000036599.15302.e5

102. Sharma PK, Mohanan N, Sidhu R, Levin DB. Colonization and degradation of polyhydroxyalkanoates by lipase-producing bacteria. Can J Microbiol [Internet]. NRC Research Press; 2019;65:461–75. https://doi.org/10.1139/cjm-2019-0042

103. Li C, Schilmiller AL, Liu G, Gyu IL, Jayanty S, Sageman C, et al. Role of β-oxidation in jasmonate biosynthesis and systemic wound signaling in tomato. Plant Cell. American Society of Plant Biologists; 2005;17:971–86. https://doi.org/10.1105/tpc.104.029108

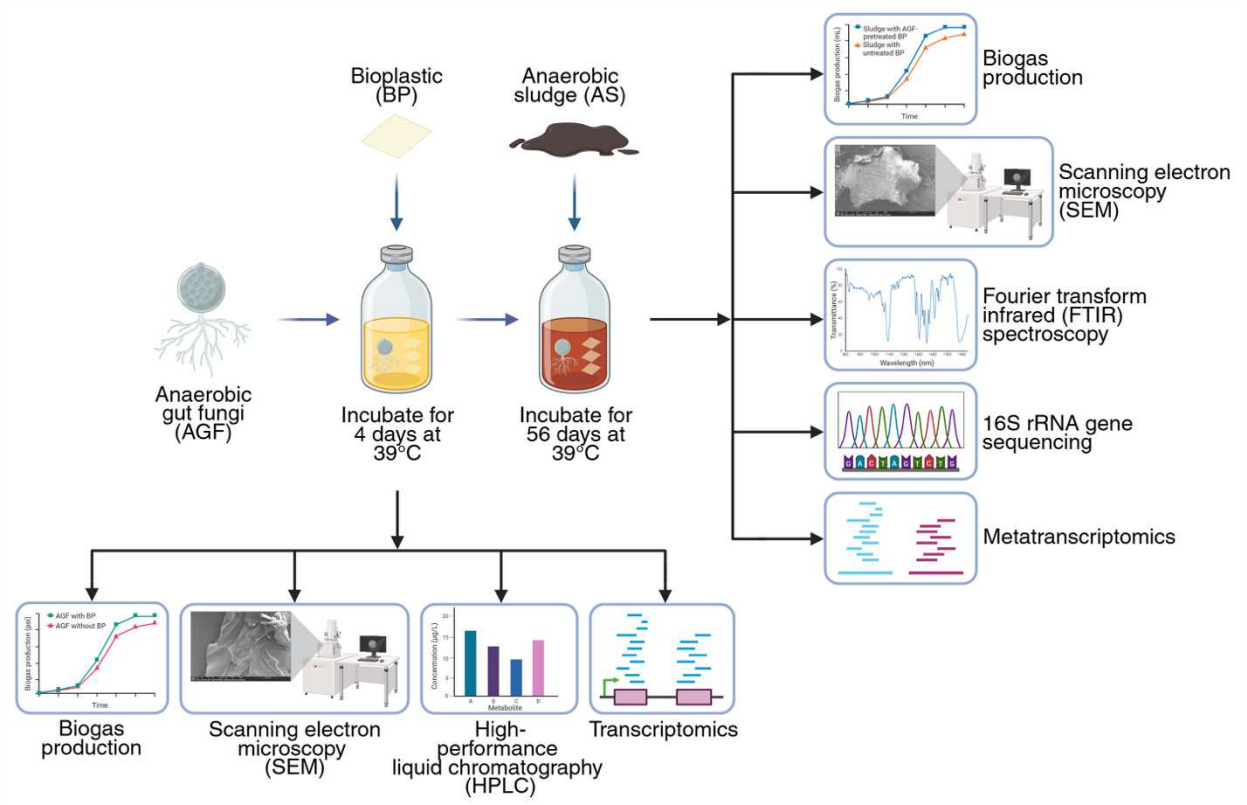


Figure 1. Schematic of the experimental design. Two species of AGF, *Neocallimastix californiae* and *Neocallimastix lanati*, were tested as fungal pretreatments on PHA, CA, and PLA BPs. PHA was pretreated by *N. californiae*, whereas CA and PLA were each pretreated by *N. lanati.* Each AGF was first grown in monoculture in MC minus medium supplemented with cellulose and its paired BP for four days. During this AGF pretreatment, biogas was measured to compare AGF growth with and without their respective BP, SEM was used to characterize AGF colonization and BP surface damage for all three AGF-BP pairings, HPLC was performed to analyze changes in metabolites during the AGF pretreatment, and the transcriptome of *N. lanati* was analyzed to identify genes driving its degradation of CA. After the AGF pretreatment, anaerobic sludge was added to the culture and incubated for an additional 56 days. Biogas production, SEM, and FTIR characterized BP degradation and surface damage for each AGF-BP pairing, while 16S rRNA gene sequencing and metatranscriptomics analyses characterized the taxonomic and gene expression shifts, respectively, that were induced by the AGF-pretreated PHA and CA. Created in https://BioRender.com.

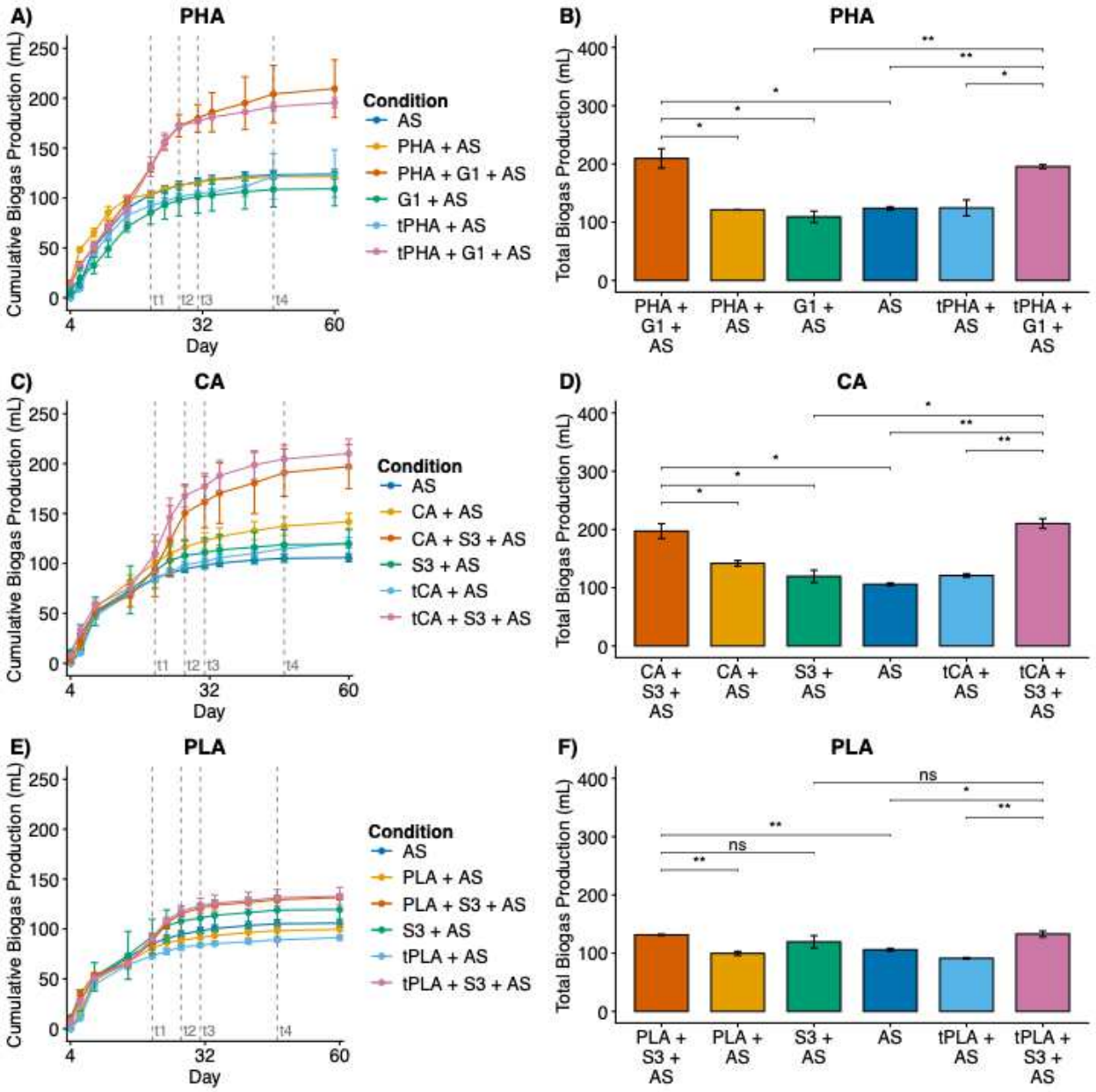


Figure 2. Biogas production from anaerobic sludge supplemented with AGF-pretreated BPs and controls. A) Cumulative biogas production of anaerobic sludge supplemented with no substrate (AS), untreated PHA (PHA + AS), G1-pretreated PHA (PHA + G1 + AS), G1 grown for four days without PHA (G1 + AS), thermally pretreated PHA (tPHA + AS), and thermally and G1-pretreated PHA (tPHA + G1 + AS). B) Statistical significance of the total biogas production for comparisons of PHA + G1 + AS and tPHA + G1 + AS to their controls, determined by Welch's t-test. Asterisks denote significant differences (* $p < 0.05$, ** $p < 0.01$, ns $p \geq 0.05$). C) Cumulative biogas production of anaerobic sludge supplemented with no substrate (AS), untreated CA (CA + AS), S3-pretreated CA (CA + S3 + AS), S3 grown for four days without CA (S3 + AS), thermally pretreated CA (tCA + AS), and thermally and S3-pretreated

CA (tCA + S3 + AS). D) Statistical significance of the total biogas production for comparisons of CA + S3 + AS and tCA + S3 + AS to their controls. E) Cumulative biogas production of anaerobic sludge supplemented with no substrate (AS), untreated PLA (PLA + AS), S3-pretreated PLA (PLA + S3 + AS), S3 grown for four days without PLA (S3 + AS), thermally pretreated PLA (tPLA + AS), and thermally and S3-pretreated PLA (tPLA + S3 + AS). F) Statistical significance of the total biogas production for comparisons of PLA + S3 + AS and tPLA + S3 + AS to their controls.

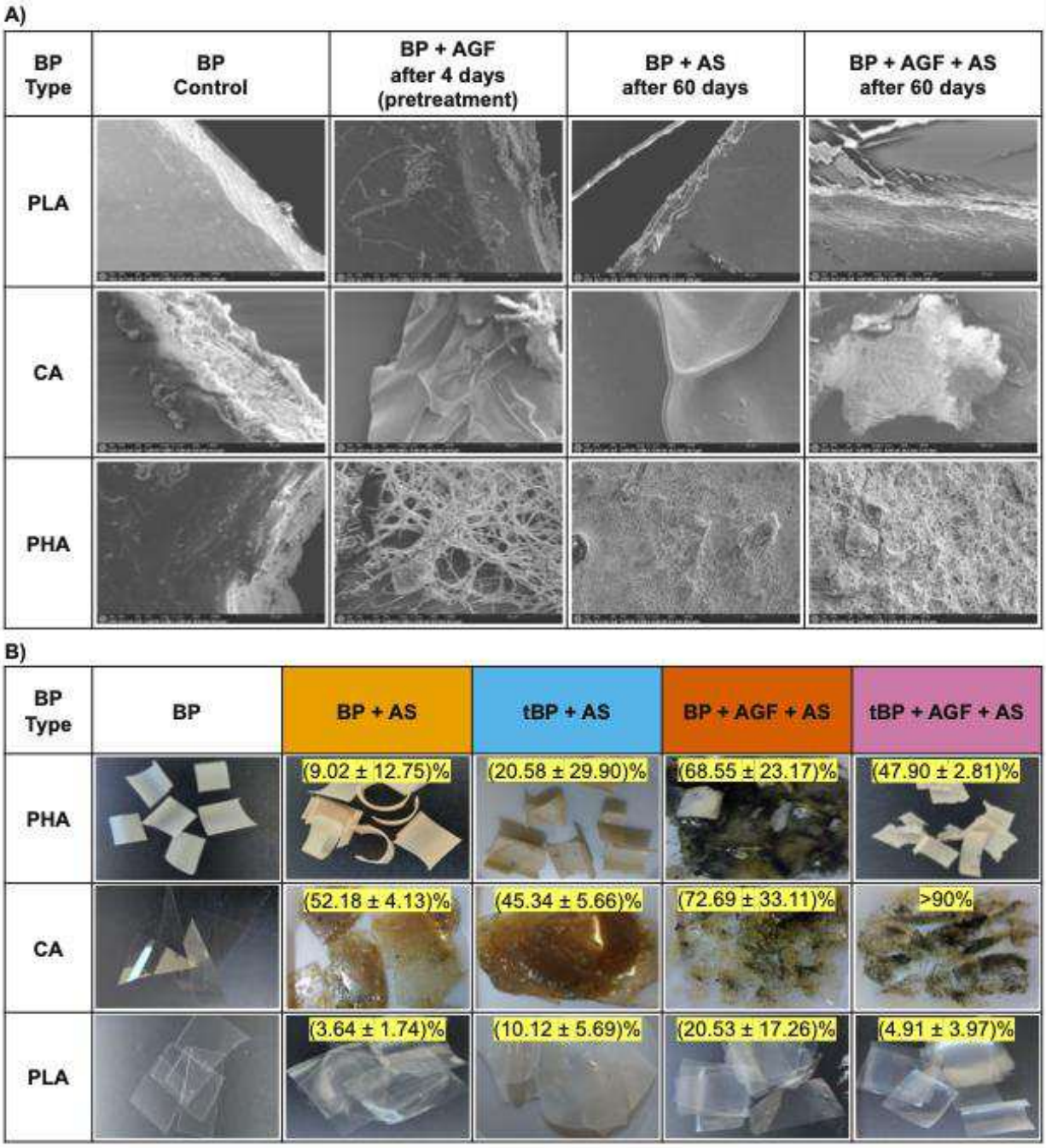


Figure 3. SEM images and weight loss measurements of untreated and AGF-pretreated BPs. A) SEM images of untreated BPs (BP), BPs after four days of AGF pretreatment (BP + AGF), untreated BPs after 56 days in anaerobic sludge (BP + AS), and AGF-pretreated BPs after four days of AGF pretreatment and 56 days in anaerobic sludge (BP + AGF + AS) for PHA, CA, and PLA BPs. B) Pictures and weight loss measurements of untreated BPs, untreated BPs after 56 days in anaerobic sludge, thermally treated BPs after 56 days in anaerobic sludge (tBP + AS), AGF-pretreated BPs after four days of AGF pretreatment and 56 days in anaerobic sludge (BP +

AGF + AS), and thermally and AGF-pretreated BPs after four days of AGF pretreatment and 56 days in anaerobic sludge (tBP + AGF + AS) for PHA, CA, and PLA BPs.

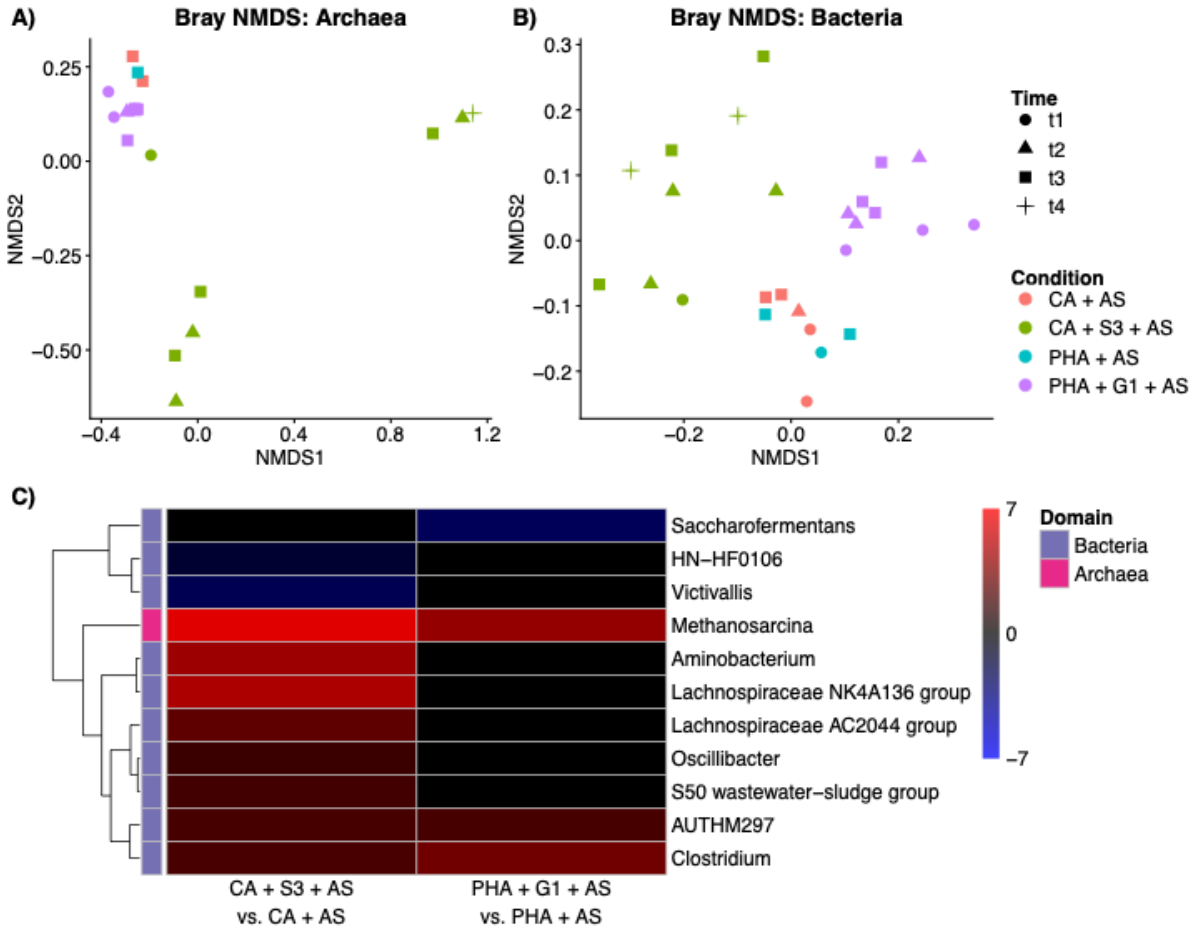


Figure 4. Taxonomic profiling of anaerobic sludge communities supplemented with AGF-pretreated BPs. Non-metric multidimensional scaling plots of Bray-Curtis dissimilarities between amplicon sequence variant (ASV) counts for A) archaea and B) bacteria in the anaerobic sludge supplemented with AGF-pretreated BPs and untreated BPs. ASV counts from the CA + S3 + AS, control CA + AS, PHA + G1 + AS, and control PHA + AS conditions were compared across 4 timepoints. C) Heatmap of bacteria and archaea that were significantly enriched ($q < 0.05$) in anaerobic sludge supplemented with the AGF-pretreated BPs in comparison to anaerobic sludge supplemented with the untreated BPs. Statistical significance was determined using ANCOM-BC2. The color scale represents natural log fold change for each comparison.

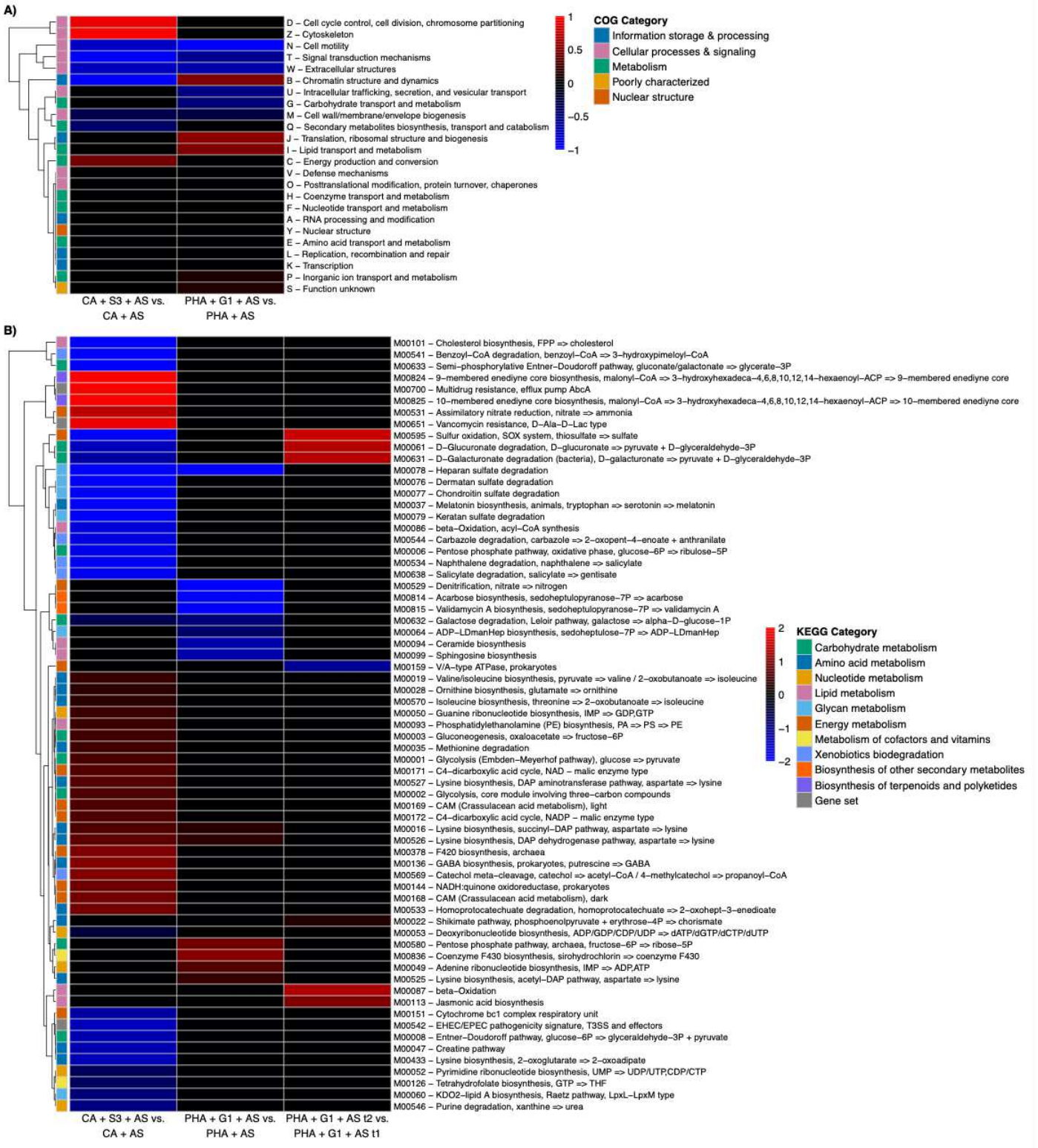


Figure 5. Metatranscriptomic analysis of metabolic functions within the anaerobic sludge microbiome supplemented with AGF-pretreated BPs. A) Heatmap showing differentially transcriptionally abundant clusters of orthologous genes in anaerobic sludge supplemented with

S3-pretreated CA compared to anaerobic sludge supplemented with untreated CA, and in anaerobic sludge supplemented with G1-pretreated PHA compared to anaerobic sludge supplemented with untreated PHA. B) Heatmap showing differentially transcriptionally abundant KEGG modules in anaerobic sludge supplemented with S3-pretreated CA compared to anaerobic sludge supplemented with untreated CA, in anaerobic sludge supplemented with G1-pretreated PHA compared to anaerobic sludge supplemented with untreated PHA, and in anaerobic sludge supplemented with G1-pretreated PHA at timepoint 2 compared to anaerobic sludge supplemented with G1-pretreated PHA at timepoint 1. Statistical significance was determined using MaAsLin2. The color scale represents the model coefficient for each comparison.

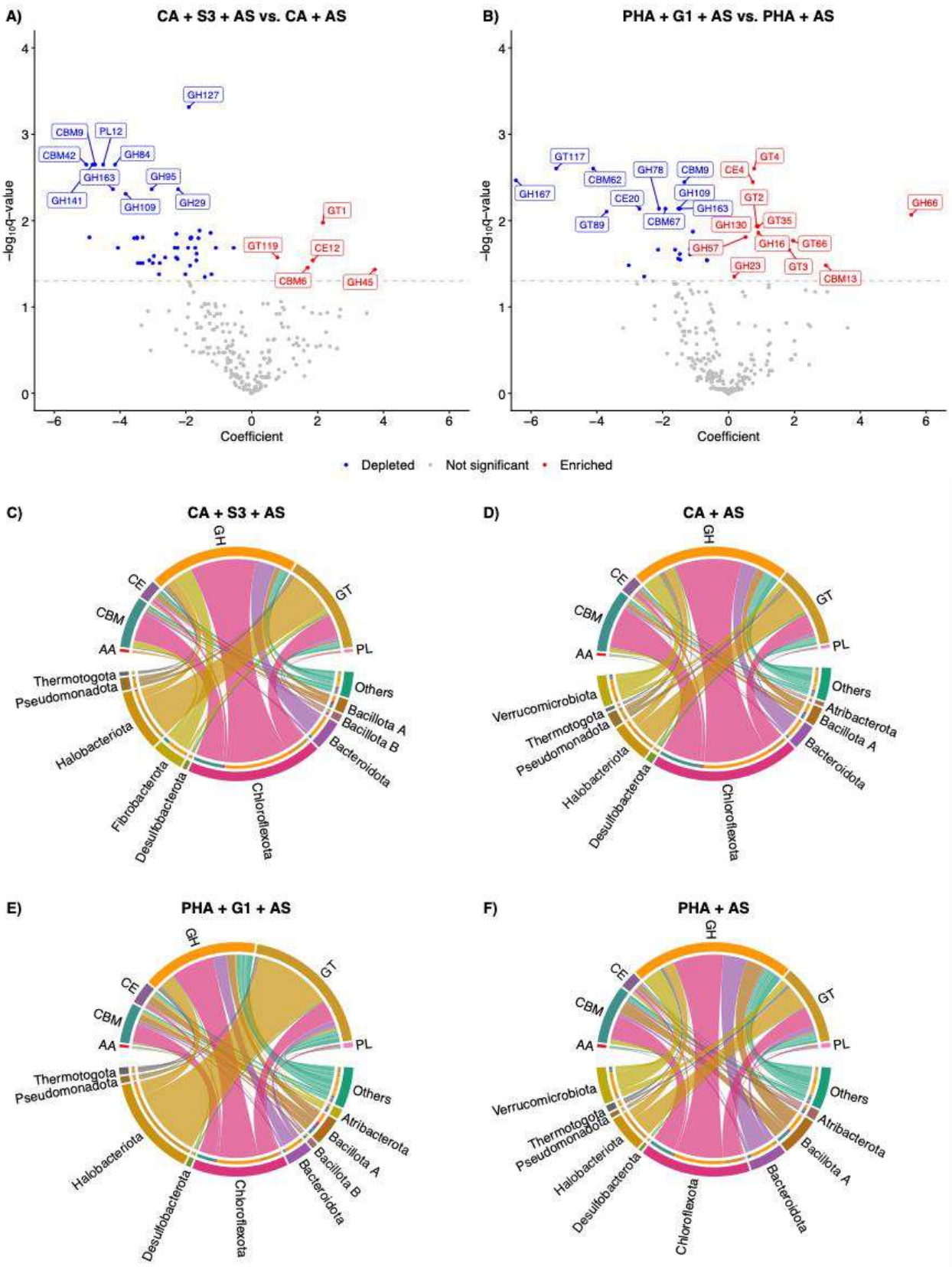

A)
CA + S3 + AS vs. CA + AS
B)
PHA + G1 + AS vs. PHA + AS
−log10q-value
Coefficient
GH127
CBM9
PL12
CBM42
GH84
GH163
GH95
GH141
GH109
GH29
GT1
GT119
CE12
CBM6
GH45
GT117
CBM62
GH78
CBM9
CE4
GT4
GH167
CE20
GH109
GT2
GH66
GT89
CBM67
GH163
GH130
GT35
GH57
GH16
GT66
GH23
GT3
CBM13
Depleted
Not significant
Enriched
C)
CA + S3 + AS
D)
CA + AS
E)
PHA + G1 + AS
F)
PHA + AS
GH
GT
CE
CBM
AA
PL
Thermotogota
Pseudomonadota
Halobacteriota
Fibrobacterota
Desulfobacterota
Chloroflexota
Bacteroidota
Bacillota B
Bacillota A
Atribacterota
Others
Verrucomicrobiota

Figure 6. Metatranscriptomic analysis of CAZymes within the anaerobic sludge microbiome supplemented with AGF-pretreated BPs. Volcano plots showing differentially transcriptionally abundant CAZyme families in A) anaerobic sludge supplemented with S3-pretreated CA compared to anaerobic sludge supplemented with untreated CA, and B) anaerobic sludge supplemented with G1-pretreated PHA compared to anaerobic sludge supplemented with untreated PHA. Statistical analysis was performed using MaAsLin2. Red labels identify all significantly enriched CAZyme families ($q < 0.05$ and model coefficient > 0) and blue labels identify the 10 most significantly depleted CAZyme families (lowest q-value and model coefficient < 0). The grey dashed line indicates the q-value cutoff, and grey dots below this line represent CAZyme families that are not significantly different ($q \geq 0.05$). Chord plots showing the top 10 phylums contributing to the 6 classes of CAZymes in anaerobic sludge supplemented with C) S3-pretreated CA, D) untreated CA, E) G1-pretreated PHA, and F) untreated PHA.

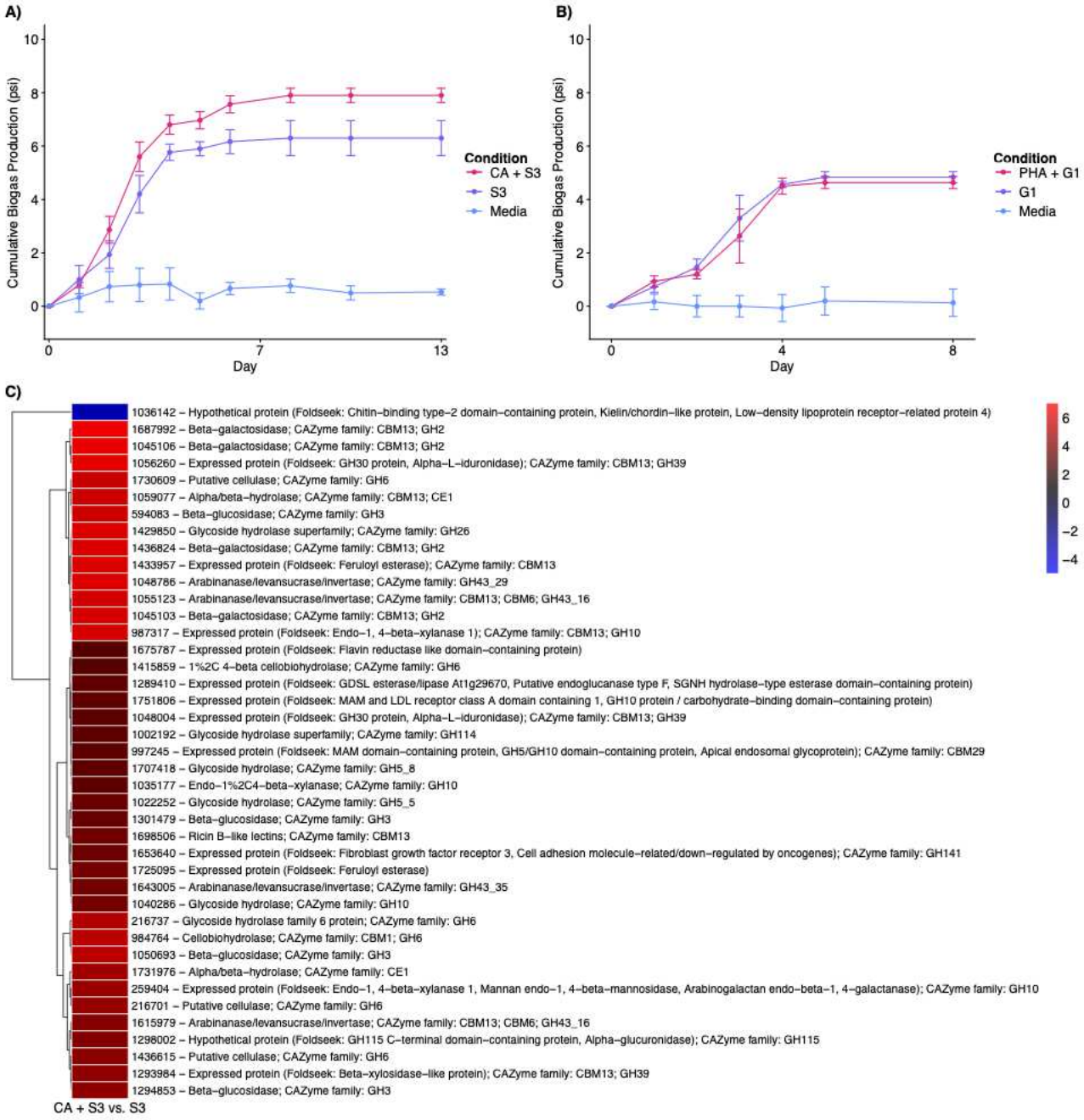


Figure 7. Impact of AGF on their corresponding BPs during the AGF-pretreatment phase. Growth curves comparing cumulative biogas production from A) *N. lanati* monocultures grown with CA to that of *N. lanati* monocultures grown without CA, and B) *N. californiae* monocultures grown with PHA to that of *N. californiae* monocultures grown without PHA. C) Heatmap of significantly differentially expressed genes in *N. lanati* monocultures grown with CA compared to *N. lanati* monocultures grown without CA. These genes have an absolute value of $\log_2$ fold change > 3 and $q < 0.01$. Genes that were annotated as "expressed protein" or "hypothetical protein" were re-annotated using Alphafold 3 and Foldseek and have "(Foldseek:"

followed by their Foldseek annotation in their label. Genes that were identified as CAZymes by dbCAN3 have "CAZyme family:" followed by their dbCAN3 annotation in their label. This heatmap highlights CAZyme genes and genes related to carbohydrate degradation activity and does not represent all of the genes that meet the abs(log_2 fold change) > 3 and q < 0.01 cutoff. The color scale represents log_2 fold change for the comparison.

Supplementary Files

This is a list of supplementary files associated with this preprint. Click to download.

- BPSupplementManuscript08192026pdffigs.docx
- SupplementaryDataset2.xlsx
- SupplementaryDataset3.xlsx
- SupplementaryDataset1.xlsx